KU LEUVEN

FACULTY OF SCIENCE

Selective adsorption of scandium with functionalized chitosan-silica hybrid materials in the context of the valorization of bauxite residue

Stijn VAN ROOSENDAEL

Promoter: Prof. Dr. Koen Binnemans

Mentor: *Joris Roosen*

Thesis presented in
fulfillment of the requirements
for the degree of Master of Science
in Chemistry

Academic year 2014-2015

Voorwoord

Het einde van mijn schoolse carrière is in zicht. Ik heb enkele mooie jaren achter de rug en ik kijk er met een voldaan gevoel op terug.

Eerst en vooral wil ik de promotor van mijn thesis, Prof. Dr. Koen Binnemans, bedanken voor zijn raad en daad. Ondanks zijn enorme drukke agenda, wist hij toch steeds hulp te bieden en raad te geven waar nodig. Mede dankzij zijn expertise in het onderzoeksveld en zijn uitvoerige feedback, wist ik mijn thesis met een goed gevoel af te ronden.

Een tweede persoon die zeker niet mag vergeten worden, is mijn mentor, Joris Roosen. Hij heeft me enorm goed opgevolgd en begeleid het afgelopen jaar en heeft me tegelijk toch ook de ruimte gegeven om te ontdekken en mijn eigen inbreng in het project te geven. Ik stel vooral zijn geduld, eerlijkheid en steun op prijs. Ook al verliep het project niet steeds zoals gewenst (wat logisch is in het onderzoeksdomein), Joris wist me steeds aan te moedigen en te motiveren. Ook was hij steeds bereikbaar als ik vragen of opmerkingen had, bijna dag en nacht.

Uiteraard is de sfeer tijdens het laboratoriumonderzoek eveneens een zeer belangrijke factor. Hiervoor zou ik graag de mede-thesisstudenten van de onderzoeksgroep van Prof. Dr. Koen Binnemans (Hendrik, Arne, Pieter, Jonas B., Jonas W. en Michiel) willen bedanken voor de leutige sfeer alsook voor de raad die ik van hen verkregen heb.

I would also like to thank Chenna for providing us with some red mud leachates, Michèle om de ICP-MS metingen uit te voeren en Dirk om de CHN metingen te voltooien.

Mijn ouders alsook mijn stiefouders, broer, stiefzussen en andere hechte familieleden waren steeds geïnteresseerd in het onderzoek dat ik verrichtte en ik dank hen dan ook voor hun steun en interesse.

Tot slot zou ik graag mijn hechte vriendengroep uit het 'Heistse' (~ Heist op den Berg) willen bedanken voor hun vriendschap. Niet alleen zorgden ze voor de nodige ontspanning tussen al het schoolwerk door, ook waren ze (vaak onbewust) van zeer groot belang om het moreel op peil te houden.

Bedankt iedereen.

Abstract (English)

The goal of this master thesis project was to selectively recover scandium from aqueous solutions by using chitosan as adsorbent. The main application of this project is the valorization of bauxite residue (*red mud*). Red mud is the byproduct of the Bayer process, which is used for the production of alumina. 90 % of the economic value of red mud originates from the presence of scandium. Being able to selectively adsorb scandium from red mud in a cheap and easy way would be of great economic importance. The main problem with the recovery of scandium from red mud, was the presence of iron. Since the ionic radius of Fe(III) ions is quite similar to the ionic radius of Sc(III) ions, their characteristics are also quite similar. Also, the concentration of iron within the red mud was significantly higher than the concentration of scandium. This is why the main focus of this master thesis project was to obtain a system with a significant higher affinity for scandium compared to iron.

In the first part of this master thesis project, some chitosan-silica hybrid materials have been synthesized (DTPA-chitosan-silica and EGTA-chitosan-silica). These materials have been synthesized in order to enhance the selective adsorption of scandium ions in comparison with iron ions. The synthesized adsorbents and the non-functionalized chitosan-silica were tested with synthetic solutions in terms of kinetics, maximum loading, pH influence and ion selectivity. Also, the reusablity of the adsorbent, the minimum acidity of the stripping solution and the efficiency of the stripping step were studied. EGTA-chitosan-silica was determined to be the most suitable adsorbent in order to gain selectivity for Sc(III).

In a second part, the functionalized chitosan-silica hybrid material that offered the most promising results, EGTA-chitosan-silica, was tested on real leachate samples of red mud.

Finally, the adsorbent was tested onto a red mud leachate in a column stripping setup since this is the setup which would be used on industrial scale. In this way, the performance of the functionalized resin material could be further investigated with regard to its separation efficiency. The scandium could successfully be separated from the iron using EGTA-chitosan-silica as an adsorbent.

Abstract (Nederlands)

Het doel van deze master thesis was om selectief scandium te herwinnen uit waterige oplossingen, gebruikmakend van chitosan als adsorbent. De voornaamste applicatie is de valorisatie van bauxiet residu (*red mud*). Red mud is een bijproduct van het Bayer proces, dat gebruikt wordt voor de productie van aluminiumoxide. 90 % van de economische waarde van red mud is afkomstig van de aanwezigheid van scandium. Het zou van enorm economisch belang zijn indien dit scandium selectief kan geadsorbeerd worden op een goedkope en eenvoudige wijze. De voornaamste moeilijkheid van het herwinnen van scandium uit red mud, was de aanwezigheid van ijzer. Aangezien de ionstraal van Fe(III) enorm gelijkaardig is aan die van Sc(III), zijn hun karakteristieke eigenschappen ook zeer gelijkaardig. Een tweede hindernis was het verschil in concentratieniveau tussen scandium en ijzer in red mud. De concentratie aan ijzer is namelijk significant veel hoger dan de concentratie aan scandium. Daarom lag de focus van deze master thesis op het verkrijgen van een systeem dat een significant grotere affiniteit heeft voor scandium in vergelijking tot ijzer. Zodoende kon er scheiding van deze twee elementen plaatsvinden.

In het eerste deel van deze master thesis werden enkele chitosan-silica hybride materialen gesynthetiseerd, namelijk DTPA-chitosan-silica en EGTA-chitosan-silica. Deze materialen werden gesynthetiseerd om zo de selectieve adsorptie van scandium in vergelijking met ijzer te verbeteren. De gefunctionaliseerde hybride materialen, alsook de niet-gefunctionaliseerde chitosan-silica partikels, werden bestudeerd gebruikmakend van synthetische oplossingen. Zo werd de kinetiek van het systeem, de maximale ladingscapaciteit, de invloed van de pH en de ion selectiviteit bestudeerd, alsook de herbruikbaarheid van het adsorbent, de minimale zuurtegraad van de stripping oplossing en de efficiëntie van de stripping stap. Er werd geconcludeerd dat EGTA-chitosan-silica het adsorbent met het meeste potentieel was om het scandium selectief te adsorberen.

In een tweede deel werd het EGTA-chitosan-silica gebruikt en bestudeerd op reële red mud leachate stalen.

In een laatste deel werd het adsorbent getest op reële red mud leachate stalen aan de hand van kolomstripping. Zo kon de efficiëntie van het scheiden van red mud mengsels via een industrieel toepasbare methode bestudeerd worden. Scandium werd succesvol gescheiden van ijzer, gebruikmakend van EGTA-chitosan-silica als adsorbent.

List of abbreviations

ATR	attenuated total reflection
CHN	Carbon Hydrogen Nitrogen
CS	chitosan-silica
DMSO-d_6	dimethylsulfoxide-d_6
DOD	degree of deacetylation
DTPA(BA)	diethylenetriamine pentaacetic acid (bisanhydride)
EDC	N-(3-dimethylaminopropyl)-N'-ethylcarbodiimide hydrochloride
EGTA(BA)	ethyleneglycol tetraacetic acid (bisanhydride)
ICP-MS	Inductively Coupled Plasma Mass Spectrometry
(FT)IR	(Fourier Transform) Infrared
NMR	Nuclear Magnetic Resonance
REE(s)	rare-earth element(s)
REO(s)	rare-earth oxide(s)
SOFC(s)	Solid-Oxide Fuel Cell(s)
TEOS	tetraethylorthosilicate
TMS	tetramethylsilane
TXRF	Total Reflection X-Ray Fluorescence

List of figures

List of tables

Content

1 INTRODUCTION

Many industrial effluents contain significant amounts of valuable metal ions. Recovery of these precious metals by adsorption would be beneficial, both for economic and sustainable reasons.[1,2] Within the last decade, a lot of research has been done to develop new and better methods for metal ion recovery from waste water streams. Especially the winning of rare-earth elements (REEs) from secondary resources has gained interest, since the REEs are more and more used in modern electronic applications.[3] As an important source of REEs, bauxite residue was considered in this thesis project. Bauxite residue, also called red mud, is the waste product resulting from the Bayer process, which is used for the production of alumina.[2,4,5] Red mud is especially rich in scandium, certainly when compared to the global scandium concentration levels. The red mud leachates that were provided for this research, originate from Greece.

The aim of this master thesis was to selectively adsorb scandium from aqueous solutions by using a chitosan-silica hybrid material. One of the main ideas was that these hybrid biosorbents could be functionalized with specific ligands in order to enhance uptake and selectivity with respect to other metal ions. Iron(III), one of the main components in red mud, was specifically targeted in the selectivity studies. First, the chitosan-silica hybrid material was synthesized by means of a sol-gel reaction. Both functionalized and non-functionalized particles were compared regarding their adsorption behavior towards scandium. The influence of a variety of parameters has been investigated to determine how adsorption capacity and selectivity could be influenced. After optimization of the parameter settings, a method has been worked out in which the adsorbent was used within a column chromatography setup.

2 RARE EARTHS

2.1 In general

The rare earths or rare-earth elements (REEs) are a group of chemically similar metallic elements (15 lanthanides, plus scandium and yttrium).[3,6,7] Despite of their name, REEs are actually not that rare.[3] Cerium for example, which is the most common REE, comprises more of the earth's crust than copper or lead.[8] Also, all of the REEs (except for promethium) are more common than mercury or silver.[8] The reason why they are called rare, is because they are naturally scattered through the earth's crust which quite often makes them economically not feasible to mine. Based on their atomic weights and their position within the periodic table, it is possible to classify these elements into light REEs (La - Sm) and heavy REEs (Eu - Lu).[3] All of them can be found in nature, in form of compounds, except promethium, which is obtained by synthetic methods.[3] Nowadays, more and more REEs are used within a variety of high-tech applications due to their unique electronic and magnetic properties (depending from REE to REE).[3] Partly because of its use in green-energy applications like hybrid cars, electric cars and wind turbines, the demand for REEs keeps on growing which also partially implies an increase in pricings.[6] In terms of volume of consumption, the most important REEs are praseodymium, cerium, yttrium, neodymium and lanthanum.[9] By 2020, the demand from the current level of 100,000 - 120,000 tons of rare-earth oxides (REOs) per year is expected to increase to 150,000 - 200,000 tons per year.[9] Also, due to the lack of ores or deposits with an economically feasible REE content, the pricing of the REEs increases even more.[3] The European Commission and the U.S. Department of Energy consider the REEs as the most critical raw materials because of its high economic importance on the one hand and its high supply risk on the other hand.[6] The latter is mainly due to the fact that China is currently producing more than 90 % of the global REE output, although this country possesses less than 40 % of the proven reserves.[3,6,9-12] Due to the introduction of strict REE export quota by China in 2011, the rest of the world was confronted with a REE supply risk.[6,11] By then, less than 1 % of the REEs were actually recycled.[6] Therefore, many research groups from other countries are trying to recycle the REEs in an economic way and hopefully develop their own rare-earth industry. Nowadays, since the REEs supply was gradually increasing while the demand was not growing as quickly as expected, a (slow) decrease in pricings is observed.[9] This is also a result of China's export policy. For example, its REE export has tightened from 50,145 tons in 2009 to

only 31,130 tons in 2012.[11] China keeps its REEs pricings low in order to avoid that REE mining in other places would become economically interesting.[7,12] This way, China keeps it quasi-monopoly on the production of REEs.[12]

2.2 Scandium

Scandium has been discovered in 1879 by the Swedish chemist Lars Fredrik Nilsson.[13] The element has been named after the only region where the minerals were found till then, namely Scandinavia.[13] Scandium is the 31st most abundant element in the Earth's crust, with an average crustal abundance of 22 ppm.[13,14] Despite this fairly common, albeit dispersed occurrence, scandium rarely concentrates in nature.[5,13,15] It does not selectively combine with the common ore-forming anions, so time and geological forces only rarely form scandium concentrations over 100 ppm.[13] Scandium can only be found in minute amounts in over 800 minerals, most commonly as a trace constituent of ferromagnesian minerals.[13,16] Within these minerals, scandium exists within its oxide form which is called *scandia* (chemical formula Sc_2O_3).[13] Scandium also concentrates in various coal deposits and basins although there is no clear explanation for this.[17]

Scandium is primarily produced as a minor element from ores exploited for other metals, since the minerals that contain appreciable amounts of scandium, such as thortveitite, euxenite and gadolinite, are rather rare.[4,13,14,16,17] Also the processing of uranium tailings and the tungsten production contribute to the scandium supply.[2,5,9] In the case of uranium wastes, high radioactivity levels make the extraction of scandium hazardous to the environment.[2] The global scandium production is about 2 tons per year in the form of scandium oxide.[14] Only about 20 % of that is from primary production while the rest of the supply originates from stockpiles made by Russia during the Cold War.[14] The principal scandium-producing countries (as a byproduct) today are China (titanium and rare earths), Russia (apatite), Ukraine (uranium) and Kazakhstan (uranium).[13,15,18] The importance of scandium will increase in the future, mainly because of its use in aluminum-scandium alloys (0.35 - 0.40 % Sc)[14] for aerospace industry components and for sports equipment such as bicycle frames, fishing rods, golf iron shafts and baseball bats.[13,15,16,18] Al-Sc alloys have got a number of superior properties including good thermal resistance, high strength with no hot cracking in welds, good resistance to corrosion, long durability and light weight.[13-15]

Another important application of scandium consists of solid-oxide fuel cells (SOFCs). The solid-oxide fuel cell industry could create a significant new demand for high-purity scandium.[9] Solid-oxide fuel cells operate at very high temperatures (~ 1000 °C) in order to make the solid electrolyte conductive.[13] The electrolyte (typically zirconia) would never withstand this temperature without being stabilized with a metal, yttria (Y_2O_3).[13] Scandia (Sc_2O_3) can substitute for yttria as a stabilizing agent for the solid electrolyte in the fuel cell.[13,19] The substitution allows reactions to occur at lower temperatures (~ 700-850 °C), extending the life of the components and increasing the power density of the unit.[13,19] This is mainly due to the fact that scandium has much better electrical conductivity than yttrium, is a superb heat-treating (and strengthening) dopant and has known applications in high-performance lighting.[13,19-21] These properties are attributed to the smaller ionic radius of Sc(III) which lowers steric blocking effects to the movement of oxygen ions.[20] Although the pricing of scandia is approximately 100 times the pricing of yttria, scandia's superior properties and attributes can outweigh the cost disadvantage.[6]

Other applications of scandium include the use of the radioactive isotope ^{46}Sc as a tracing agent in oil refineries[15,16], the use of scandium sulfate in order to improve the germination of seeds[16], the use of scandium iodide in mercury vapor lamps in order to replicate sunlight within the television industry[9,13,16], the use of scandium within military equipment[9], the use of scandium as an analytical standard[15], the use of scandium in electronic components[15] and the use of scandium as a recyclable Lewis acid catalyst for the production of fine chemicals[11]. The price of scandium(II)oxide, with over 99.95 % purity, costs about € 6500/kg.[22] This high pricing is the consequence of its scarcity and to the rather complicated metallurgical processes necessary for its recovery and purification.[15]

A general scheme of the production process of scandium metal is shown within Figure 1.

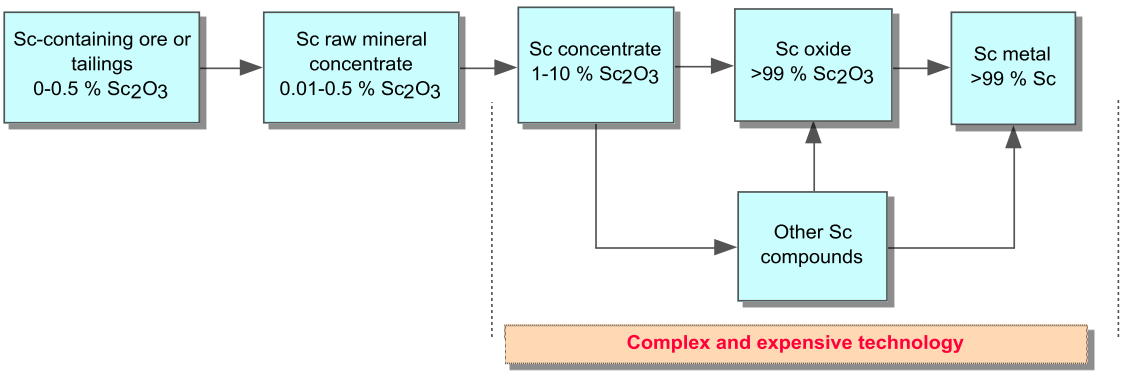

Figure 1: General production scheme of scandium[9]

Because of its scarcity, recovery of scandium from secondary resources should also be considered, besides its primary mining. Scandium is especially present in red mud, the main waste product of the Bayer process.[4] Aluminium metal is electrochemically produced from alumina (Al_2O_3) using the Hall-Héroult process.[23] The Bayer process on its turn is used for the refining of bauxite[1] to alumina.[23,24] Red mud is an insoluble residue primarily composed of iron oxides, quartz, sodium aluminosilicates, calcium carbonate/aluminate and titanium dioxide.[2,4,23] Many minor elements are present in the residue of which scandium, together with the other rare earths, are the most valuable ones.[2,4] The major elements within the red mud sample are shown within Table 1.

Table 1: Main elements within red mud.[25]

Compound	Wt%
Fe_2O_3	44.6
Al_2O_3	23.6
CaO	11.2
SiO_2	10.2
TiO_2	5.7
Na_2O	2.5

Due to the fact that the Bayer process is a cyclic process, most of the REEs are accumulated and enriched within the red mud with each cycle of the process.[5,23] Red mud is considered to be harmful waste when it is stockpiled in huge amounts, partially because of the fact that the red mud pulp has a pH of about 12.[2,4,23,25] Also, the huge

[1] named after Les Baux, the district in France where the ore was first mined

tailing ponds occupy vast land areas which cannot be used for other applications in this way. For every ton of alumina produced, between 1 and 2 tons of red mud residues (dry weight) are produced.[23] Seen its current production rate, being 120 million tons a year, it is not that remarkable that 2.7 billion tons of red mud has already been stockpiled in the past.[4,11,25] Valorization of this waste product therefore imposes itself. 95 % of the economic value of red mud arises from the presence of scandium.[11] The ability to adsorb scandium from aqueous (waste) solutions in an effective way could be of great economic and environmental interest.[26,27] Red mud tailings typically contain 50 - 110 ppm scandium, but the red mud in Greece for example contains 105 - 156 ppm scandium.[4,13] If this amount is converted to the 2.7 billion tons of waste currently stockpiled, a huge amount of more than 280 tons of scandium is available within this waste product. Because of the commercial value of scandium, which depends on the purity of the metal, it is important to separate scandium in a high purity form from the main elements present in red mud.[26] The main problems of the adsorption are the low scandium content and the selectivity towards the other major elements present in red mud.[4] Especially the high abundance iron(III) is a problem since the ionic radii of scandium(III) and iron(III) are quite similar and so is their chemical behavior.[26,27]

The metals within the red mud are extracted by acidic dissolution (leaching).[2,11] Some procedures to separate scandium from the other elements already exist. These procedures are mostly based on ion exchange separation by cation, anion or chelating exchangers, on liquid membrane technology or on solvent extraction techniques.[5,15] Liquid membrane technology is a technique for the separation of solutes in double-emulsion systems.[15] The main advantage of this method is the high transport efficiency in comparison with the conventional liquid-liquid extraction.[15] Most of the disadvantages concerning liquid membrane technology are related to the instability of the emulsion itself, resulting in re-mixing of the feed and receiving phases.[15] Solvent extraction with organic solvents is the most common technology to separate and purify scandium from solutions with large amounts of impurity elements since it has the advantages of ease of operating at large scales and high extraction capacities.[15] However, the risk of contamination of the aqueous streams with organic solvents and extractants is big by using solvent extraction procedures, which is disadvantageous in terms of a sustainable, zero-waste concept.[28] The current ion exchange separation procedures have some disadvantages such as slow exchange reaction rate, poor recyclability of the ion

exchanger resin, not being applicable for many working cycles and a high cost of the ion exchange resin.[5,15,28]

3 CHITOSAN AS AN ADSORBENT

3.1 Chitosan

The most widely applied adsorbent is activated carbon but its high price makes using it less beneficial in terms of economics, especially in industrial applications.[29] Therefore, development of alternative adsorbents has been under intensive study in recent decades.[29] Within the framework of this master thesis, the use of chitosan is investigated to selectively adsorb scandium from aqueous solutions. Chitosan is a linear polysaccharide which is mainly obtained by alkaline deacetylation of chitin, a naturally abundant organic material.[1,28,30,31] Chitin can be found in the exo-skeleton of crustacea (such as lobsters and shrimps), insects, fungi and other non-vegetable organisms, mostly besides minerals and proteins.[30-35] It is therefore the second most abundant polysaccharide found in nature, after cellulose.[28,36,37] To give an idea of the natural chitin production: it is estimated that 10 billion tons of chitin is synthesized by nature each year.[31] Since crustacean shells are waste products of seafood processing industries, chitin is an ideal, low-cost material to start from.[32] Both chitin and chitosan are high molecular weight polymers of glucose linked by β-(1,4) glycosidic linkages.[31] In the commercial and scientific areas, chitosan is usually attributed to products of chitin which exhibit rates of deacetylation higher than 60 % and a nitrogen content higher than 7 %.[31,32] During the production of chitosan, different parameters within the production process can be varied. These variations alter the chemical characteristics of the synthesized chitosan, with the degree of deacetylation (DOD) as the most important one.[31] The DOD has a direct effect on the chemical reactivity, the biodegradability and the solubility of the chitosan since the amine groups are much more reactive than the acetamide groups.[1,31]

A simple representation of the reaction is shown within Scheme 1.

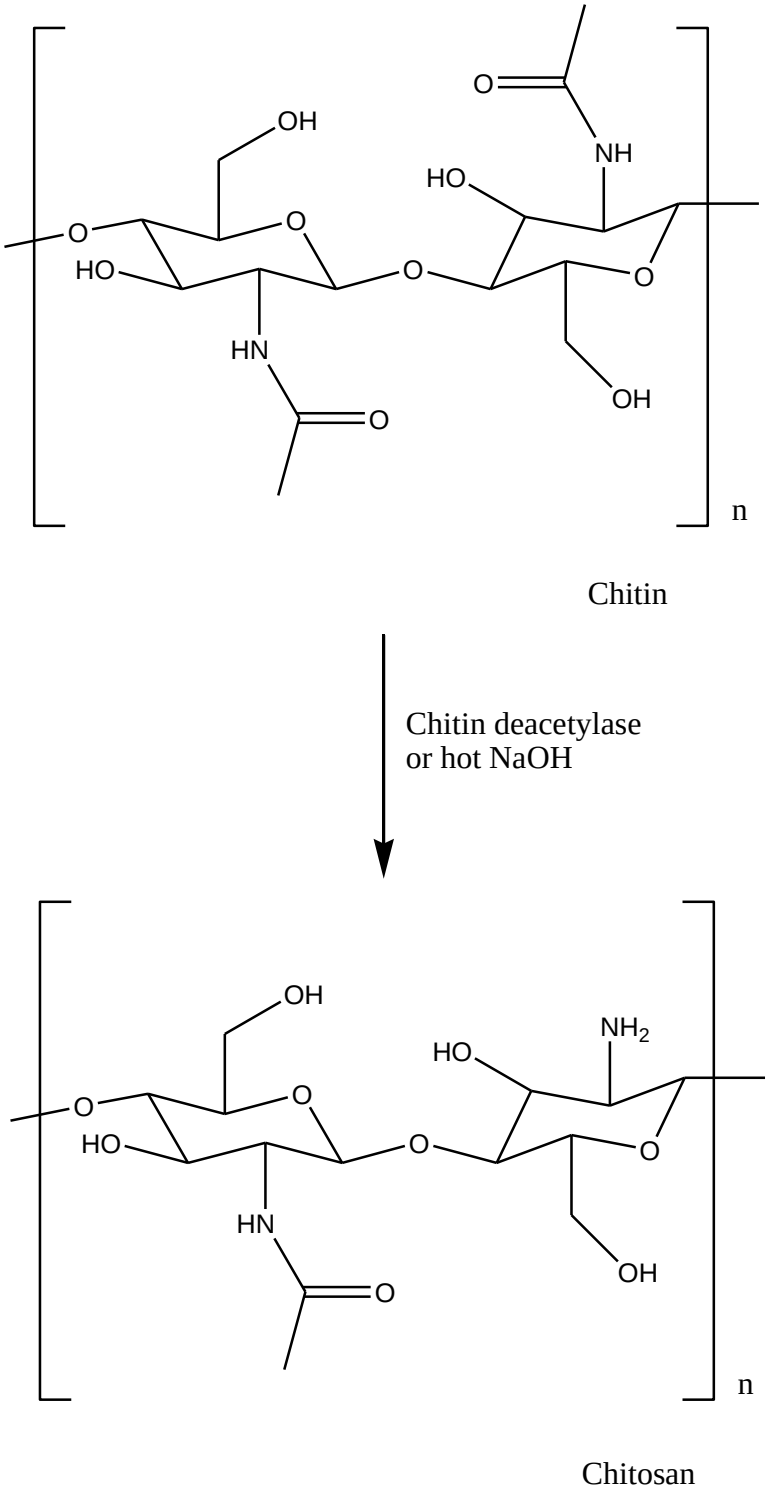

Scheme 1: Synthesis of chitosan from chitin

Since isolation of chitin out of crustacean shells is the most common method, only this method will be discussed. Other possibilities are the extraction of chitin out of insects or

out of fungi.[31] Three types of chitin can be identified, namely α-chitin, β-chitin and γ-chitin.[1,31,37] The type of chitin which is present in the shells of crustacean is α-chitin, which corresponds to an antiparallel arrangement of the polymer chain.[37] The isolation of chitin out of crustacean shells consists of three steps: deproteinization, demineralization and decolorization.[31] The proteins are firstly removed from the shells by treating them with mild sodium hydroxide or potassium hydroxide solutions (between 1 % and 10 % w/v) at slightly elevated temperatures (30 °C to 100 °C) for 30 min to 12 h.[31,37] Calcium phosphate, calcium carbonate and other mineral salts are then extracted with dilute acids (= demineralization).[31] Decolorization is done by mixing the chitin with acetone.[38]

The free electron doublet of nitrogen on amine groups is responsible for the sorption of metal cations.[39] Chitosan is therefore an excellent natural adsorbent for metal ions with much higher selectivity and loading capacity than usual commercial chelating resins.[40,41] Chitosan becomes a polyelectrolyte in acidic medium due to the protonation of NH_2-groups.[42] The following equilibrium describes the state of ionization[42]:

$$\mathrm{Chit-NH_2 + H_3O^+ \rightarrow Chit-NH_3^+ + H_2O} \quad (1)$$

This indicates that competition for available adsorption sites will arise at low pH values between metal ions and protons.[29] This results in a decrease of adsorption efficiency.[29] On the other hand, when working at high pH values, hydrolysis of the metal ions could take place. The hydrolysis characteristics of scandium(III) can best be explained by the presence of three hydrolysis products: $[Sc(OH)]^{2+}$, $[Sc_2(OH)_2]^{4+}$ and $[Sc_3(OH)_5]^{4+}$.[43,44] Hence, the pH is a very important parameter when investigating the adsorption characteristics of the chitosan-silica material.

The affinity of chitosan for cations does not depend on the physical form of the chitosan (either as a powder, a film or in solution).[1] Also, the particle size does not have any significant influence on the saturation adsorption capacity and an increase in temperature decreases the saturation adsorption capacity of chitosan.[1,32] The excellent adsorption characteristics of chitosan as such were considered to be due to the following factors:

1. The high hydrophilicity of chitosan owing to large number of hydroxyl groups.[40]
2. The large number of primary amino groups with high activity as adsorption sites for metal ions.[1,40] In acidic solutions, these amine groups are protonated and

could easily attract anionic metal compounds (resulting from metal chelation by anionic ligands).[28]

3. The flexible structure of the polymer chain of chitosan which enables to adopt the suitable configuration for complexation with metal ions.[40]

Not only the adsorption characteristics are of great interest to many researchers, also the low cost, the abundancy, the biocompatibility, the biodegradability, the anti-bacterial activity, the non-toxicity, the cellular compatibility and its solubility at acidic pH values (unlike chitin)[32] are interesting characteristics.[28-33,45] The large number of primary amino groups and hydroxyl groups with high reactivity enable a variety of chemical modifications.[28,40]

3.2 Chitosan-silica

Since pure chitosan suffers from poor mechanical properties and low chemical resistance, it needs to be hybridized with another material (for example with silica) in order to be useful on an industrial scale.[30,41,46,47] Chitosan combined with silica has been shown to be suited as a supporting material for column chromatography.[47] Organic-silica polymeric materials combine the functional properties of the polymer with the hardness of silica.[48] Hybridization can be done using an in-situ sol-gel hybridization method.[30,46,48] It has been demonstrated that the chitosan-silica hybrid material is well-suited as a resin material for column chromatography because of its excellent mechanical resistance, the large surface area and the high porosity of the material.[29,46]

3.3 Functionalized chitosan-silica

Chitosan has been functionalized with many ligands.[49-52] These functionalization processes can be used for controlling the reactivity of the polymer or enhancing sorption kinetics (controlling diffusion properties for example).[39] Analogously, the chitosan-silica hybrid can be functionalized by grafting ligands on the amine groups of the chitosan moieties. In this work, chitosan-silica was modified by immobilization of two different functional groups: diethylenetriamine pentaacetic acid (DTPA) and ethyleneglycol tetraacetic acid (EGTA), which are shown within Figure 2.

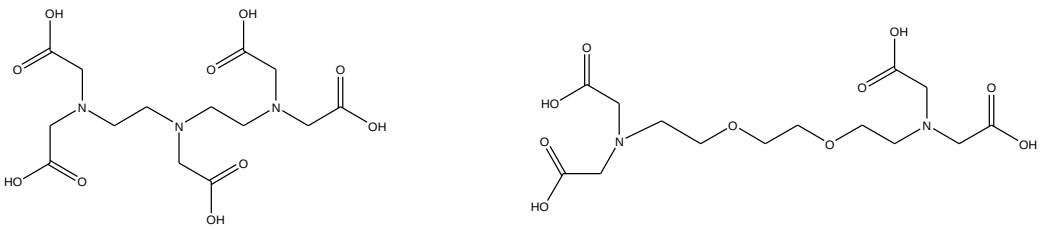

Figure 2: Structures of DTPA (left) and EGTA (right)

The grafting of carboxylic functions (present within the DTPA or the EGTA ligands) enhances the adsorption of rare earths compared to non-functionalized chitosan.[1,28,40] DTPA and EGTA are chosen within this thesis project as these ligands form stable complexes with scandium.[53] When chitosan is functionalized, the adsorption of metals takes place at a much lower pH compared to regular, non-functionalized chitosan.[32]

4 TECHNIQUES, EQUIPMENT AND REAGENTS

4.1 Reagents

Tetraethyl orthosilicate (≥ 99.0 % pure) was purchased from Merck KGaA (Darmstadt, Germany).

Chitosan (≥ 99.0 % pure) was purchased from Sigma-Aldrich (Diegem, Belgium).

$Fe(NO_3)_3 \cdot 9H_2O$ (≥ 99.0 % pure) was purchased from J.T. Baker Chemicals B.V. (Beventer, Holland).

$Sc(NO_3)_3 \cdot xH_2O$ (99.99 % pure) was kindly supplied by Stanford Materials Corporation (Irvine, California, USA).

Hydrochloric acid (~ 37 %), ethanol (99.99 %) and sodium sulfite anhydrous (analytical reagent grade) were purchased from Fischer Scientific U.K (Loughborough, UK).

Ammonia (25 w%), n-heptane (99+ %), nitric acid (65+ %), gallium standard (990-1010 µg/mL ± 0.4 %), lanthanum standard (990-1010 µg/mL ± 0.3 %), cerium standard (1000 µg/mL ± 2 µg) and holmium standard (990-1010 µg/mL ± 0.4 %) were purchased from Chem-Lab NV (Zedelgem, Belgium).

Serva silicon solution was purchased from SERVA Electophoresis GmbH (Heidelberg, Germany).

Acetic acid (100 %) and sodium hydroxide (min 97.0 %) were purchased from VWR International (Heverlee, Belgium).

Pyridine (99+ %), methanol (99.99 %), acetic acid anhydride (99+ %), sulfuric acid (96 %) and diethylenetriamine pentaacetic acid (98+ %) were purchased from Acros Organics (Geel, Belgium).

Ethyleneglycol tetraacetic acid (Ultra pure grade; 97.0 %) was purchased from Amresco Inc (Solon, Ohio, USA).

Hydroxylamine hydrochloride (99+ %) was purchased from Riedel-de Haën (Seelze, Germany).

N-(3-dimethylaminopropyl)-N'-ethylcarbodiimide hydrochloride (99 %) was purchased from Fluorochem (Hadfield, UK).

All products were used as received, without further purifications.

The bauxite residue, precursor of the red mud leachates which have been studied in this work, was provided by the Aluminum of Greece Company, which is located at Agios Nikolaos, Greece.

4.2 Techniques and equipment

4.2.1 Fourier Transform Infrared spectroscopy (FTIR)[54]

Infrared (IR) spectroscopy is a method to deduct the structure of a sample by irradiating the sample with infrared (IR) radiation and measuring the radiation which is transmitted (or absorbed) by the sample. The sample absorbs radiation when the frequency of the radiation is equal to the frequency of the vibrations between the atoms of the sample. A spectrum which indicates the intensity versus the frequency of an absorption peak is generated. Since every structure has his own unique spectrum, the spectrum can be compared to a molecular fingerprint of the sample. Not only does the spectrum give information about which molecule(s) is/are present, also the amount of material present is indicated by the size of the absorption peaks.

Fourier Transform Infrared spectroscopy (FTIR) is an infrared spectral analysis technique where an interferometer is used. Most interferometers employ a beamsplitter which divides the incoming beam into two separate beams. One beam reflects off of a flat mirror of which the position is fixed. The other beam reflects off of a flat mirror which can move over a short distance in order to increase the path of the beam. These two beams are recombined and are actually interfering which each other at which a signal called an 'interferogram' is created. This interferogram has the unique property that each data point has information about all the frequencies at once. FTIR is preferred over dispersive or filter methods of infrared spectral analysis since it can measure all of the infrared frequencies simultaneously, rather than individually, which has several advantages being the most important ones the speed of the scans and the sensitivity of the measuring method. Since a spectrum is needed where each individual frequency has got its own intensity, some kind of mathematical 'decoding' needs to be deducted which is called 'Fourier transformation'.

FTIR spectra were measured on a *Bruker Vertex 70 FTIR spectrometer* that gives access to the mid–IR and far–IR spectral ranges down to 400 cm^{-1}. Measurements were done on a platinum ATR (attenuated total reflection) device.

4.2.2 Total Reflection X-ray Fluorescence spectroscopy (TXRF)[55]

The main principle of X-ray Fluorescence spectroscopy is that atoms, when irradiated with X-rays, emit secondary X-rays which is called fluorescence radiation. Since the wavelength and energy of the fluorescence radiation is specific for each element, an overview of which elements are present within the sample can be made. The concentration of each element present can be calculated using the intensity of the fluorescence radiation in comparison with the intensity of a known standard.

The X-ray beam is generated typically by a molybdenum tube and is reflected on a multilayer monochromator resulting in a monochromatic X-ray beam. This small beam impinges on the sample holder carrying the sample. XRF uses an angle of incidence of 45 ° while TXRF uses a very small angle of incidence (< 0.1 °) in order to irradiate the sample, causing total reflection of the beam. This reduces the absorption as well as the scattering of the beam in the sample matrix. The fluorescence radiation is detected by an energy-dispersive detector and the intensity is measured using an amplifier coupled to a multichannel analyzer. Using TXRF results in a significant reduction of matrix effects and a greatly reduced background noise by which much higher sensitivities are obtained.

Prior to analysis, a sample preparation has to be done. A known amount of a certain standard solution (1000 mg/L) is added to an Eppendorf tube along with a known amount of a metal ion aqueous solution and diluted to a total of 1 mL with Milli-Q waterChoice of the proper standard solution depends on the energy level of the characteristic secondary X-rays emitted by the element of interest. This mixture is then stirred well in order to homogenize the solution. In order to gain the most accurate results, the concentration level of the added standard should be as close as possible to the concentration level of the metal to be measured. 2 µL of this stirred sample is then put on a clean quartz plate which has been pre-coated with Serva, a hydrophobic silicon solution, to avoid spreading of the sample droplet. The quartz plate is dried in an oven at a temperature of 60 °C.

The TXRF apparatus which has been used within this master thesis was a *Bruker S2 Picofox* with a molybdenum source.

4.2.3 Inductively Coupled Plasma Mass Spectrometry (ICP-MS)[56-58]

ICP-MS is a very sensitive technique which can detect elements within the sub-ppb concentration level. Within an ICP-MS apparatus, a sample is injected in a high-temperature ICP torch which ionizes the sample. These ions are then separated using a mass spectrometer.

In order to generate ions, the sample is injected in liquid form into a spray chamber with a nebulizer. The sample emerges as an aerosol and moves to the base of the plasma. As it continues its path true the plasma, the sample is dried, vaporized, atomized and eventually ionized. These ions are then led to the mass analyzer. The plasma torch itself is made by using argon gas. Argon gas flows inside the concentric channels of the ICP torch. Oscillating electric and magnetic fields are established at the end of the torch. When a spark is applied to the argon flowing through the ICP torch, electrons are stripped of the argon atoms resulting in argon ions. These ions are caught in the oscillating field and collide with other argon atoms, creating an argon discharge or plasma.

The ICP-MS apparatus which has been used during this master thesis was a *Thermo Scientific X Series ICP-MS* with Cell Collision Technology. It uses a Quadrupole mass analyzer setup.

4.2.4 CHN elemental analysis[59-62]

CHN elemental analysis is based on the 'principle of Dumas' which involves complete and instantaneous oxidation of a sample by flash combustion in an oxygen-rich environment. In the combustion process, carbon is converted to CO_2, hydrogen to H_2O and nitrogen to N_2. The generated combustion products are swept out of the combustion chamber using an inert gas such as argon or helium and are passed over heated high-purity copper. The copper removes any oxygen not consumed in the initial combustion process and converts any oxides of nitrogen to nitrogen gas. Other combustion products can also be generated (due to the presence of chlorine or so) but these are removed thanks to a variety of adsorbents. The combustion products (CO_2, H_2O and N_2) are then separated by a chromatographic column and detected by a thermal conductivity detector which gives an output signal proportional to the concentration of the individual components of the mixture. One of the main advantages of this method is that only 2-3 mg of sample are needed in order to conduct the analysis.

The CHN elemental analysis has been carried out using a *CE instruments EA-1110 CHN element analyzer*.

4.2.5 Column setup

A column experiment has been conducted by using a Büchi fraction collector B-684 with a Büchi chromatography pump B-688. The dimensions of the column are 9.6 mm x 115 mm, which implies a bed volume of 8.3 mL.

4.2.6 Nuclear Magnetic Resonance spectroscopy (NMR)[63-65]

The recording of an NMR spectrum is based on the presence of a nonzero spin of nuclei within a certain sample. Isotopes which have an odd number of protons and/or neutrons have got such a nonzero spin and are NMR active. The nuclei of the sample possess both a magnetic moment as an angular momentum.

The nuclei of the sample are subjected to a constant, external magnetic field by which the randomly oriented nuclei align themselves with the magnetic field. This creates a splitting of the energy levels of the nuclei at an alpha and at a beta level. The initial population of a certain energy level is determined by thermodynamics, as described by the Boltzmann distribution, by which the alpha level (lower energy) is preferred to the beta level (higher energy). The irradiation of the nuclei with a superimposed electromagnetic field results in a change in transition from the alpha to the beta level. The nuclei of the higher energy state return to the lower energy state (= relaxation) whereby energy is emitted true electromagnetic radiation which has the same energy as the energy difference between the two energy levels. The fluctuation of the magnetic field associated with the relaxation process is called resonance and this resonance can be detected by a receiver coil and converted into an NMR spectrum. Peaks at different frequencies can be detected due to the fact that different nuclei are shielded or deshielded differently by small local fields generated by the electrons around the nucleus. Adjacent non-equivalent nuclei can couple to one another which generates splitting patterns. After analyzing the number of peaks, the area under each peak (integration), the splitting pattern of each peak and the position of each peak (chemical shift), the chemical structure of the sample can be deduced.

Chemical shifts are expressed in ppm and referenced to tetramethylsilane (TMS). Dimethylsulfoxide-d_6 (DMSO-d_6) was used as solvent to make the product soluble enough (also filtered through a syringe filter to be sure not having undissolved solid particles in the NMR tube). Solvent residual signals for DMSO-d_6, were observed as a quintet signal at 2.50 ppm in the ^{1}H NMR spectra.[66] For the same reason, a predominant heptet signal could be observed at 39.51 ppm in the ^{13}C NMR spectra.

All ^{1}H NMR and ^{13}C NMR spectra were recorded on a *Bruker Avance 300 spectrometer* with autosampler (operating at 300 MHz for ^{1}H NMR and 75 MHz for ^{13}C NMR).

4.3 Health, safety and environment

In order to protect yourself and the environment, some strict regulations need to be followed concerning the experiments. In general, a lab coat and safety goggles are mandatory when entering a laboratory. Other protection equipment can also be needed, depending on the chemicals used and the techniques involved in the experiments.

Every experiment which has been conducted, has been studied in detail up front by filling in a risk assessment. These risk assessments contain important information such as which chemicals will be used, which risks are connected to these chemicals, which reaction(s) and possible side-reaction(s) can occur, which glassware and laboratory equipment will be used, which techniques will be used, etc... These risk assessments then need to be approved by a health and safety coordinator of the chemistry department before starting the experiments. The health and safety coordinator checks whether the right necessary precautions have been taken such as wearing the right protection equipment (safety goggles, lab coat, gloves, ...) and handling the chemicals in a right and safe way (by working underneath a fume hood for example).

Special care was taken when working with methanol due to its flammability as even a small amount of methanol can be lethal when swallowed. The smallest amount reported to cause death is 15 mL of 40 % methanol.[67] Therefore, this product has been classified as risk class E4 with clearance by KU Leuven which implies that an extended risk assessment had to be filled out.

In the adsorption tests using the column setup, a maximum pressure of 15 bar was set on the chromatography pump in order to avoid breaking of the material and possible explosion of the glass chromatography column was avoided.

5 SYNTHESIS

5.1 Synthesis of chitosan-silica hybrid material

A chitosan-silica hybrid material was made according to the method described by Rashidova et al.[48] by dissolving chitosan (2.0 g) in a 2 vol% acetic acid solution (100 mL). After the chitosan was dissolved (after approximately 1 h), tetraethylorthosilicate (TEOS, 30 mL) was added to the pale yellow viscous solution. The solution, which was at pH 4.00, was stirred for another 30 min to induce the hydrolysis reactions during which ethoxy groups are replaced by hydroxyl groups. Afterwards, the pH was sufficiently increased by adding 200 mL of a solution of 3 vol% NH_3 to catalyze the condensation reactions. The mixture was kept for about 24 h during which the chitosan-silica interpenetrating networks were formed. Then, the chitosan-silica hybrid material was filtrated and washed with demineralized water until the pH reached a neutral value. Consequently, the chitosan-silica hybrid material was washed again with ethanol to replace water in the chitosan-silica gel with ethanol. This facilitates the drying afterwards since ethanol evaporates much faster to air in contrast to water. To end the washing procedure, the chitosan-silica gel was washed with *n*-heptane (300 mL), which acts as an antisolvent and hence the chitosan-silica particles precipitate. The chitosan-silica gel was then air-dried for a period of 24 h and dried further in vacuum at an elevated temperature of 40 °C for another 24 h. The result of this procedure is a dry, white-colored powder.

The formation of the chitosan-silica hybrid material, starting from chitosan and TEOS, is depicted in **Fout! Verwijzingsbron niet gevonden.**.

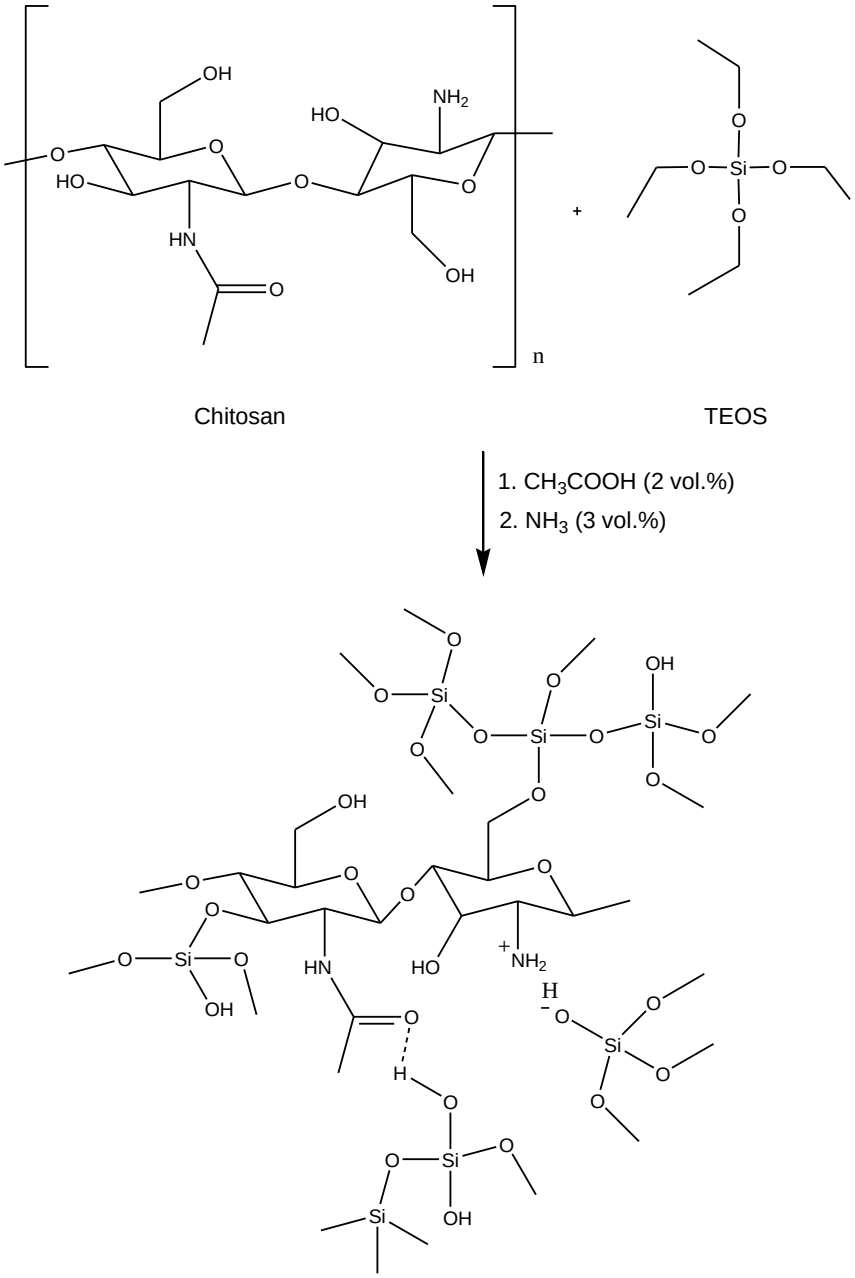

Scheme 2: Reaction of chitosan and TEOS

In total, five batches of chitosan-silica have been synthesized. Each time (10.2 ± 0.8) g of the chitosan-silica hybrid material was obtained.

An IR study was conducted onto the (dried) chitosan-silica. The characteristic peaks of the sample are summarized below:

IR (ATR, cm^{-1}): 3366 (broad bend; O-H stretch + N-H stretch), 1653 (C=O stretch amide), 1559 (C-N stretch), 1069 (Si-O-Si symmetric stretch), 966 (Si-O stretch silanol).

Also, a CHN study has been conducted onto the chitosan-silica samples. The measured carbon content was (8.09 ± 0.06) %, the hydrogen content was (2.82 ± 0.03) % and the nitrogen content was (1.37 ± 0.03) %. No percentages could be calculated up-front since it is impossible to know the exact structure of the chitosan-silica molecules. The measured percentages were quite consistent through the different batches. As can be seen, the percentages are way lower than the percentages for pure chitosan (C: 40.19 %, H: 6.27 and N: 7.25 %), which indicates the presence of inorganic silicon atoms.

5.2 Synthesis of precursors for functionalization

Diethylenetriamine pentaacetic acid bisanhydride (DTPABA) was made starting from DTPA (19.7 g), acetyl anhydride (20.4 g) and pyridine (23.7 g) as a solvent.[68] The reaction was done at an elevated temperature of 65 °C, with a reflux condenser and under argon atmosphere in order to minimize the water content. After two hours, the reaction was stopped and the product was immediately filtrated, washed three times with acetyl anhydride (approximately 70 mL) and dry diethyl ether (20 mL). Afterwards, the DTPABA was dried under vacuum conditions at an elevated temperature of 40 °C for 24 h. The reaction scheme is shown in Scheme 3.

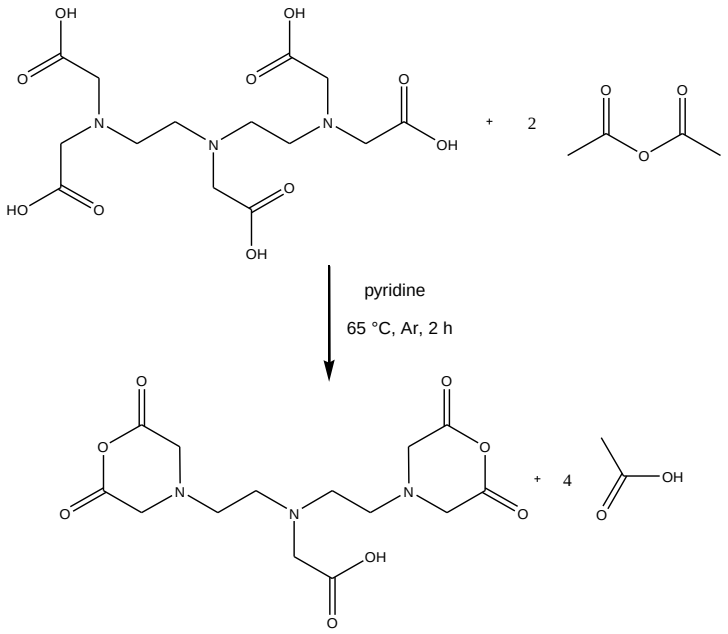

Scheme 3: Synthesis of DTPA-bisanhydride

In total, two batches of DTPABA have been synthesized. The color of the substance was yellowish-white and it had some larger particles in it. These larger particles were crunched into smaller ones in order to homogenate the particle size. The yield of the reaction was (98.7 ± 0.8) %.

An NMR study has been conducted on the DTPABA sample in order to check it for impurities. The results of the ^{1}H NMR study of DTPABA are:

^{1}H NMR (300 MHz, DMSO-d_6, δ ppm): 2.59 (t, J = 6.15 Hz, 4H, CH_2-C**H**$_2$-N-CH_2-COOH); 2.75 (t, J = 6.15 Hz, 4H, C**H**$_2$-CH_2-N-CH_2-COOH); 3.30 (s, 2H, C**H**$_2$-COOH); 3.71 (s, 8H, C**H**$_2$-CO-O-CO).

The result has been double checked by also conducting a CHN study. The measured carbon content is (45.79 ± 0.16) %, the hydrogen content is (4.79 ± 0.19) % and the nitrogen content is (11.28 ± 0.00) %. The calculated values, based on the structure of the DTPABA, are a carbon content of 47.06 %, a hydrogen content of 5.36 % and a nitrogen content of 11.76 %.

The measured values are quite constant. Since the average values are a little bit lower than the calculated values, a conclusion can be made that traces of water are probably present within the bisanhydride.

The results of the IR-study of the DTPABA are:

IR (ATR, cm^{-1}): 1771 (symmetric C=O stretch anhydride), 1637 (C=O stretch carboxylic acid), 1330 (C-O stretch), 1105 (C-N stretch), 943 (O-H bend).

The second precursor, ethyleneglycol tetraacetic acid bisanhydride (EGTABA), was synthesized using the same method as DTPABA. The reaction scheme of the EGTABA synthesis is shown within Scheme 4.

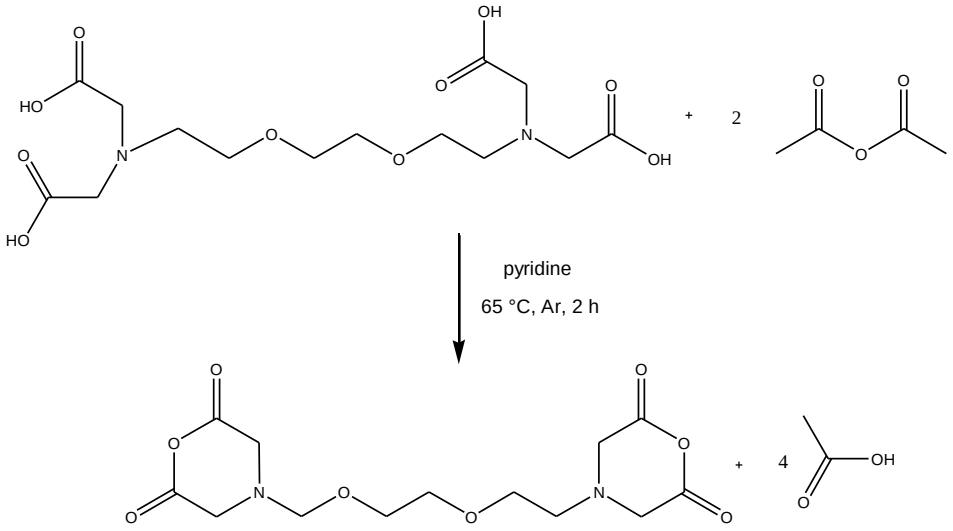

Scheme 4: Synthesis of EGTA-bisanhydride

The functionalization process of EGTABA started with 100 mmol of EGTA. The EGTABA was dried under vacuum conditions and at an elevated temperature (40 °C) for 24 h. The bigger particles were crunched into smaller ones in order to homogenate the particle size. The average yield of the two batches was (40.5 ± 2.4) %.

An NMR study has been conducted on the first batch of the EGTABA sample in order to check it for impurities.

The results of the ^{1}H NMR study of EGTABA are:

^{1}H NMR (300 MHz, DMSO-d_6, δ ppm): 3.47 (t, J = 6.15 Hz, 4H, O-C**H**$_2$-CH$_2$-N); 3.45 (s, 4H, C**H**$_2$-O-CH$_2$-CH$_2$-N); 2.82 (t, J = 6.15 Hz, 4H, CH$_2$-C**H**$_2$-N-CH$_2$-CO-O); 2.09 (s, 8H, CH$_2$-N-C**H**$_2$-CO-O).

The result has been double checked by also conducting a CHN study. The measured carbon content is (40.16 ± 0.03) %, the hydrogen content is (6.16 ± 0.08) % and the nitrogen content is (6.94 ± 0.01) %. The calculated values, based on the structure of the DTPABA, are a carbon content of 48.84 %, a hydrogen content of 5.85 % and a nitrogen content of 8.14 %.

The measured values are very much the same. When looking at the results, one can see that the H content is too high while the C and N contents are too low. Since anhydrides are very hygroscopic, it is most likely that the difference within the measured values in comparison with the calculated values is due to the presence of water.

The results of the IR-study of the EGTABA are:

IR (ATR, cm^{-1}): 3048 (C-H stretch), 1728 (symmetric C=O stretch anhydride), 971 (C-N stretch).

When comparing the IR spectrum with the results of the IR spectrum of pure EGTA, one can see that the peak of the O-H stretch at 3423 cm^{-1} and the peak of the C=O stretch (carboxylic acid) at approximately 1630 cm^{-1} have disappeared. A conclusion can be made that the EGTABA synthesis has been successful.

5.3 Functionalization of the hybrid material

The functionalization of the chitosan-silica hybrid material with DTPA has been carried out by mixing chitosan-silica (7.5 g) in 2.0 vol% acetic acid solution (100 mL) and stirring it in order to catalyze the reaction between the DTPABA and the amino-groups of chitosan. DTPABA (15.0 g) was dissolved in pure methanol (100 mL). After adding more methanol (400 mL) to the chitosan-silica mixture to act as a solvent, the dissolved DTPABA was also added to the mixture and stirred in order to start the functionalization process. After 24 h, the stirring was stopped and a 0.20 M NaOH solution (100 mL) was added in order to raise the pH. The mixture has to be approximately at pH 11.00 in order to remove the excess DTPA by formation of its sodium salt. A pH value of 11.00 was reached by gradually adding more pellets of NaOH to the mixture. The alkaline mixture has been washed with demineralized water (200 mL), HCl 0.10 M (200 mL) and again with demineralized water until the pH reached neutral. After that, the DTPA-chitosan-silica material was washed with ethanol (200 mL) in order to facilitate the drying process by replacing water with ethanol (better evaporation to air). After drying in a vacuum oven, the particles were stored in contact with the air in order to equilibrate its water content with the water content of the air. A total of (9.5 ± 0.5) g of DTPA-chitosan-silica was obtained.

The results of the IR study of the DTPA-chitosan-silica are:

IR (ATR, cm^{-1}): 3366 (broad bend; O-H stretch + N-H stretch), 1636 (C=O stretch amide), 1397 (symmetric vibration COO), 1065 (Si-O-Si stretch).

A conclusion can be made that the functionalization was effectively conducted.

The functionalization of the chitosan-silica hybrid material with EGTA has first been carried out by following the same method used for functionalization with DTPA. This method for the synthesis of EGTA-chitosan-silica consisted of a combination of two existing procedures.[69,70] Since the functionalization of chitosan-silica with EGTABA seemed not to work, another method has eventually been applied.[69] In this method, chitosan-silica (7.5 g) was added to EGTA (3.2 g) and dissolved in demineralized water (100 mL). In order to dissolve the mixture a bit better, the mixture was heated till 60 °C and stirred for 4 h. After the heating and stirring, the mixture has been cooled down to 40 °C after which 1.00 M NaOH (10 mL) and N-(3-dimethylaminopropyl)-N'-ethylcarbodiimide hydrochloride (EDC, 2.0 g) were added in order to initiate the gelation of the mixture. EDC is a water soluble cross-linking agent that activates carboxyl groups for the coupling of primary amines. The mixture was stirred for 1 h at 40 °C after which the mixture was stirred for 16 h at room temperature. The gel was washed with acetic acid 5 m% (50 mL). A MeOH-AcOH-Ac_2O 4:2:1 5 % solution (140 mL) was added and stirred for 3 h. The gel was successively washed with 0.10 M NaOH, demineralized water, 0.10 M HCl, demineralized water and n-heptane. Since filtration of the slurry took a huge amount of time, the washing steps have been carried out by centrifuging the slurry multiple times. Since centrifuging couldn't remove all of the moisture without spilling functionalized particles, the last washing step has been conducted by doing a (time consuming) filtration. The washed EGTA-chitosan-silica has been dried for 24 h at 60 °C in vacuum. A total of 7.5 g of EGTA-chitosan-silica was obtained.

The results of the IR study of the EGTA-chitosan-silica are:

IR (ATR, cm^{-1}): 3359 (broad bend; O-H stretch + N-H stretch), 1653 (C=O stretch amide), 1419 (COO symmetric vibration), 1074 (Si-O-Si stretch).

The EGTA-chitosan-silica has also been studies using the CHN method. The measured carbon content is (11.02 ± 0.06) %, the hydrogen content is (3.74 ± 0.05) % and the

nitrogen content is (1.85 ± 0.01) %. Since the N content increased, compared to pure chitosan-silica (1.85 % compared to 1.37 %), a conclusion can be made that EGTA is present within the structure.

A conclusion can be made that the functionalization has been successful.

6 ADSORPTION EXPERIMENTS

6.1 Preparation of the stock solutions

6.1.1 Synthetic stock solutions

To start the adsorption experiments, some stock solutions have been made. 500 mL of a 5.00 mM $Fe(NO_3)_3 \cdot 9H_2O$ solution was made by weighing $Fe(NO_3)_3 \cdot 9H_2O$ and dissolving it into milliQ water. The same has been done for $Sc(NO_3)_3 \cdot 5H_2O$ in order to make a Sc(III) stock solution. A TXRF study has been conducted in order to check the exact molarity of the stock solutions. In order to minimize external parameters, the pH of the stock solutions has been set to equal values by adding some HNO_3. In order to avoid hydrolysis of the metal ions, the stock solutions were acidified. From the solubility constants, it was calculated that, at a concentration of 0.50 mM, Fe(III) precipitates as $Fe(OH)_3$ at pH 2.4 and Sc(III) precipitates as $Sc(OH)_3$ at pH 4.1.[71] This has to be avoided as these precipitates do not bear any charge and will therefore not be adsorbed to the adsorbent. Taking into account the pH increase of one unit by a tenfold dilution of the stock solution in order to perform the actual batch experiments, it was decided to adjust the pH of the stock solution to pH 1.00, using HNO_3.

The metal ion concentrations were determined by TXRF. The Fe(III) stock solutions contained 5.04 mM of Fe(III) and the Sc(III) stock solution contained 4.83 mM of Sc(III).

Also, a stock solution of Fe(III) and Sc(III) within sulfate medium has been made using the same method as for the preparation of the stock solution within nitrate medium. The only differences were the weighed salt masses and the use of H_2SO_4 in order to increase the acidity of the solution. The concentration of the Fe(III) stock solution was 6.31 mM and the concentration of the Sc(III) stock solution was 4.88 mM.

By mixing the monocomponent solutions of Fe(III) and Sc(III), binary mixtures could be obtained. The Fe(III)/Sc(III) binary stock solution within nitrate medium had an Fe(III) content of 2.50 mM and a Sc(III) content of 2.25 mM. The Fe(III)/Sc(III) binary stock solution within sulfate medium had an Fe(III) content of 3.41 mM and a Sc(III) content of 2.02 mM.

6.1.2 Red mud samples

The sample was dried at 105 °C for 12 h. Next, the material was passed through a 500 µm size mesh before it was used in leaching studies. The leaching of the bauxite residue was carried out in sealed polyethylene bottles by constant agitation using a laboratory shaker (Gerhardt Laboshake) for 24 h at 160 rpm and 25 °C. The leaching experiments were carried out with a 0.20 M acid solution with liquid to solid ratio of 50:1. The chemical composition within the bauxite residue (not the leaching solutions) are shown within Table 2 and Table 3.

Table 2: Main elemental composition of the Greece bauxite residue (measured using 'Wavelength Dispersive X-ray Fluorescence Spectroscopy')

Compound	wt. %
Fe_2O_3	44.6
Al_2O_3	23.6
CaO	11.2
SiO_2	10.2
TiO_2	5.7
Na_2O	2.5

Table 3: REEs concentration within the Greece bauxite residue (measured using ICP-MS)

Element	Concentration (g/ton)	Element	Concentration (g/ton)
Sc	121 ± 10	Gd	22.0 ± 1.9
Y	75.7 ± 9.6	Tb	3.5 ± 0.6
La	114 ± 15	Dy	16.7 ± 0.7
Ce	368 ± 68	Ho	3.9 ± 0.6
Pr	28.0 ± 3.9	Er	13.5 ± 1.8
Nd	98.6 ± 7.0	Tm	1.9 ± 0.3
Sm	21.3 ± 2.3	Yb	14.0 ± 1.9
Eu	5.0 ± 0.9	Lu	2.4 ± 0.3

6.2 DTPA-chitosan-silica as adsorbent

6.2.1 In general

The adsorption experiments concerning the different parameters were conducted in batch mode. The batch experiments started by taking 10 mL of a solution with a certain solution, potentially adapting the pH value of the solution by adding a known amount of acid/base, adding a certain amount of DTPA-chitosan-silica and a magnetic stirrer and stirring the solution at 300 rpm using a magnetic stirrer. In order to minimize variables within the experiments, the adsorbent is added to the vials at the same time. After

reaction has taken place for a certain amount of time, the solutions were filtrated using a 0.45 µm polypropylene syringe filter. This way, the adsorbent has been separated from the solution and no more adsorption could take place. The remaining metal ion content within the solution has been measured by using a TXRF apparatus since it is rather difficult to determine the amount of ions adsorbed onto the functionalized chitosan-silica itself. The adsorption amount could then be calculated using the following formula:[1,29,72]

$$q = \frac{c_0 - c_{eq}}{m} \times V \quad (2)$$

In this formula, q is the amount of adsorbed metal ion (mg/g adsorbent), c_0 is the initial metal ion concentration (mg/L), c_{eq} is the equilibrium metal ion concentration (mg/L), m is the adsorbent mass (g) and V is the volume of the solution (L).

6.2.2 Influence of different parameters

Some parameters were investigated in batch mode in order to explore which parameters gave the best adsorption values and selectivity. First of all, the kinetics were investigated. This has been done by diluting the stock solution until the Fe(III) and/or Sc(III) concentration was 0.50 mM. (25.0 ± 0.5) mg of adsorbent was added to each reaction. After a preset time period, the solutions were filtrated.

The influence of the adsorbent mass was also investigated. For this experiment, the stock solutions of Fe(III) and Sc(III) have been diluted to 2.50 mM. After addition of different adsorbent masses to the diluted metal ion solution (10 mL), adsorption took place for 4 h in order to reach equilibrium conditions.

Thirdly, the influence of the pH on the adsorption characteristics has been determined. This has been done by diluting the stock solutions until the Fe(III) and/or Sc(III) concentrations were 0.50 mM. Notice that the initial pH values differed for the monocomponent solutions compared to the binary solution. The pH values were properly adjusted by adding concentrated HNO_3 (or concentrated H_2SO_4 when working within sulfate medium) to make the solution more acidic and by adding NaOH 4 M to make the solution more alkaline. After setting the pH values to 0.00, 0.50, 1.00, 1.50, 2.00, 3.00, 4.00 and 5.00, 25.0 mg of the adsorbent has been added. The adsorption lasted 4 h before the adsorption experiment was stopped by filtration of the biosorbent particles. When calculating the adsorbed metal content, a proper volume correction was taken into

account since the adaptation of the pH values included the addition of a certain volume of acid or base.

A fourth and last parameter which has been investigated is the effect of the sulfate concentration on the adsorption characteristics of non-functionalized chitosan-silica particles. This has only been done for the solutions within sulfate medium since metal ions may form complexes with sulfate ions to form negative sulfate complexes, which is not the case with nitrate ions. Negatively charged sulfate complexes are expected to be adsorbed by the positively charged non-functionalized chitosan-silica molecules since the amine groups of non-functionalized chitosan-silica are positively charged when the pH value is below 6.00.

6.2.2.1 Influence of the adsorbent mass

With the adjusted stock solutions, the influence of the adsorbent mass was investigated. One needs to know the amount of adsorbent needed to obtain full recovery. In order to obtain more accurate results, adsorption was in this case performed from aqueous solutions with a higher concentration compared to the following adsorption experiments. The metal ion concentration was 2.50 mM instead of 0.50 mM usually. The data plot is shown within Figure 3. It can be observed that all ions were adsorbed from both the Sc(III) and Fe(III) solution when 100 mg of adsorbent was added to the 2.50 mM solution. An assumption can be made that at least 20.0 mg of adsorbent is necessary to adsorb all ions from a 0.50 mM solution. In order to be sure to obtain 100 % recovery of the Sc(III) ions present in solution, it was decided to use 25.0 mg of adsorbent for all following adsorption experiments.

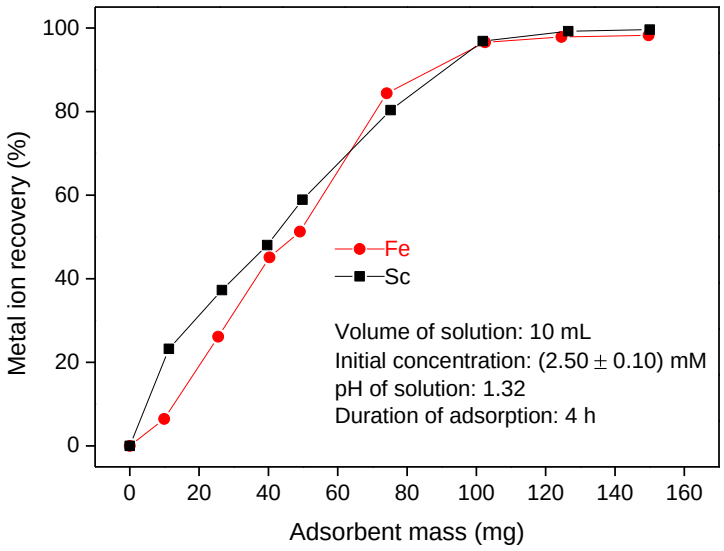

Figure 3: Results of the influence of the adsorbent mass on the adsorption of the Sc(III) and Fe(III) ions (nitrate medium - DTPA-chitosan-silica as adsorbent)

6.2.2.2 Kinetics

A kinetics experiment is conducted by adding 25.0 mg of adsorbent to 10 mL of a 0.50 mM Fe(III) or Sc(III) solution. This routine was repeated 8 more times within a certain time frame (ranging from 5 minutes to 6 h). In this way, one can decide which time frame is necessary to reach equilibrium conditions. The results of the kinetics experiment within nitrate medium, using DTPA-chitosan-silica as adsorbent, are shown within Figure 4. As can be seen, after approximately 2 h of adsorption, equilibrium conditions are reached for both iron and scandium adsorption. Just to make sure, the minimum adsorption time for all following adsorption experiments has been determined to be 4 h. It should also be mentioned that a slightly higher adsorption amount is observed for Sc(III) than for Fe(III).

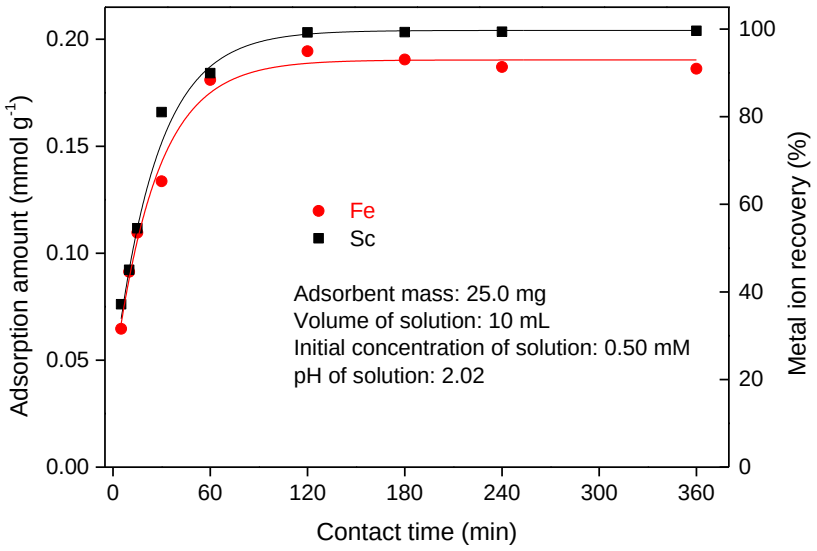

Figure 4: Results of the kinetics experiment of the Sc(III) and Fe(III) diluted stock solution (nitrate medium - DTPA-chitosan-silica as adsorbent)

6.2.2.3 Influence of the pH

The influence of the pH onto the Sc(III) and Fe(III) adsorption was investigated by adjusting the pH values of the stock solutions to pH 0.00, 0.50, 1.00, 1.50, 2.00, 3.00, 4.00 and 5.00. 25.0 mg of DTPA-chitosan-silica was added to the solutions with different pH and the mixtures were stirred for 4 h. The Sc(III) and Fe(III) ions which were still present after adsorption took place, were measured using a TXRF apparatus. The exact amount of adsorbed ions can only be calculated when the hydrolysis reaction of Fe(III) and Sc(III) is taken into account. Otherwise, a wrong assumption is made that all of the ions have been adsorbed without any presence of hydrolysis. The results of the pH influence, without taking into account the hydrolysis reaction, are shown within Figure 5.

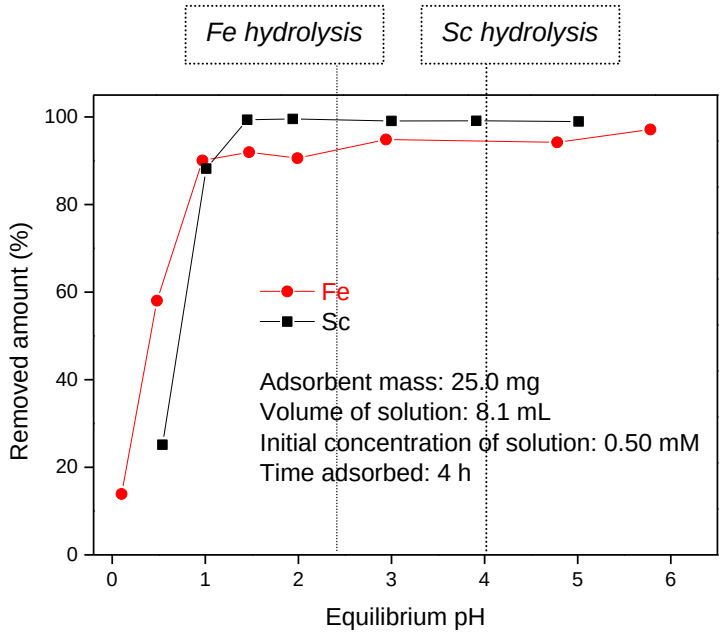

Figure 5: pH influence on the Fe(III) and Sc(III) adsorption (nitrate medium - DTPA-chitosan-silica as adsorbent)

Figure 5 shows that there is a small difference in ion adsorption of Fe(III) and Sc(III) by the DTPA-chitosan-silica. Since the stability constant of DTPA-Fe(III) (28.60)[73] is higher than the stability constant of DTPA-Sc(III) (27.43)[74], it is likely that the ion adsorption starts at lower pH values for the Fe(III) solution, as can be seen within Figure 5.

Also, when comparing Figure 4 and Figure 5, a conclusion can be made that the adsorption affinity and adsorption capacity are different for Sc(III) and Fe(III). The adsorption affinity of DTPA-chitosan-silica for Sc(III) may be lower than the adsorption affinity of DTPA-chitosan-silica for Fe(III), but the adsorption capacity seems to be higher for Sc(III) in contrast to Fe(III). This hypothesis is supported by Figure 3. The difference in adsorption capacity for Fe(III) and Sc(III) decreases by adding more adsorbent, which implies a higher availability of adsorption sites, is used. Thus, the adsorption capacity is slightly higher for Sc(III) than for Fe(III) in a more competitive environment. A possible explanation for the higher adsorption capacity for scandium could be that the non-functionalized amine groups also interact with the cations. At pH values below pH 1.00, the amine groups are protonated which indicates an electrostatic repulsion towards the scandium and iron cations. At somewhat higher pH values, the amine groups are neutral (no charge) which indicates no electrostatic repulsion towards the cations. The free electron pair of the amine group can coordinate with scandium and/or iron. If the (non-

functionalized) amine groups have a preference for scandium cations instead of iron cations, it is possible that the adsorption capacity is higher for scandium than for iron.

The pH influence was also investigated in a binary mixture of Fe(III) and Sc(III) by diluting the binary stock solution 10 times (so a concentration of approximately 0.25 mM of both Sc(III) and Fe(III) was achieved) and adjusting the pH values to values varying from 0.00 to 5.00. After letting the equilibrium set in, 25.0 mg of DTPA-chitosan-silica was added to the solution and the adsorption experiment lasted for 4 h. Since the data plot of the binary mixture is quite similar to the data plot from the two separate Fe(III) or Sc(III) stock solutions (Figure 5), the data plot of the binary mixture is not shown. A conclusion can be made that the pH is a very important parameter when looking at adsorption characteristics.

In order to gain some more info relating the selectivity of the two different ions (Fe(III) and Sc(III)), the binary stock solution was diluted only 5 times (to a concentration of approximately 0.50 mM for both Sc(III) and Fe(III). In this way, the selectivity of the Fe(III) and Sc(III) can be investigated more clearly to one another. As can be seen within Figure 6, the Fe(III) ions are preferentially adsorbed. This is due to the greater stability constant of the DTPA-Fe(III) (28.60)[73] in contrast to the stability constant of the DTPA-Sc(III) (27.43).[74] At pH 2.00 and rising, a sudden increase for Fe(III) is observed from approximately 85 % to nearly 100 % of Fe(III) removed, which is due to the formation of $Fe(OH)_3$. For Sc(III), the adsorption is gradually increased until pH 3.00, which implies that no Sc(III) hydrolysis is present. This implies that there is a difference in adsorbed amount between scandium and iron. After studying the hydrolysis reaction (see next topic), a correct assumption about the ongoing processes can be made.

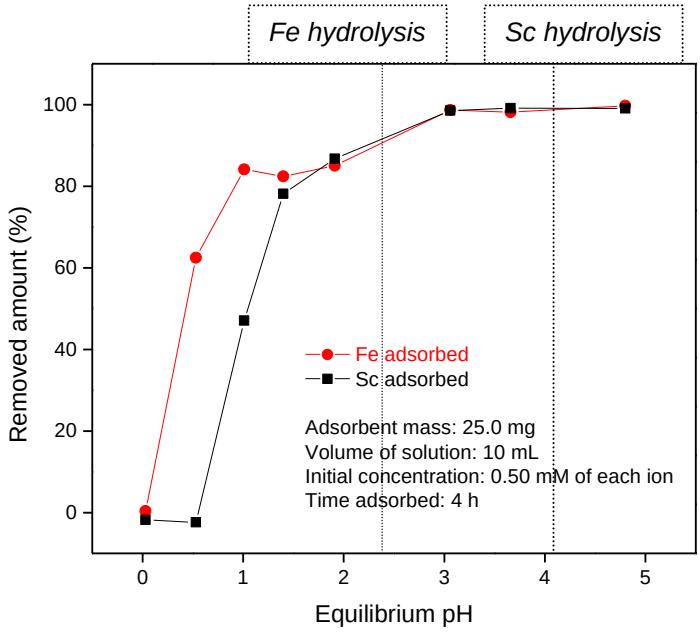

Figure 6: pH influence on the Fe(III)/Sc(III) adsorption within a binary mixture of Fe(III) and Sc(III), 0.50 mM (nitrate medium - DTPA-chitosan-silica as adsorbent)

6.2.2.4 Hydrolysis

In order to quantify the hydrolysis processes, 0.50 mM Fe(III) and Sc(III) solutions have been used. The pH values were adjusted from pH 0.00 to 5.00. The solutions were stirred overnight in order to ensure equilibrium conditions for the hydrolysis reactions. Multiple filtrations were necessary to be sure that all precipitates were completely removed from solution. After measuring the remaining Fe(III) and Sc(III) content within this solutions, Figure 7 could be created.

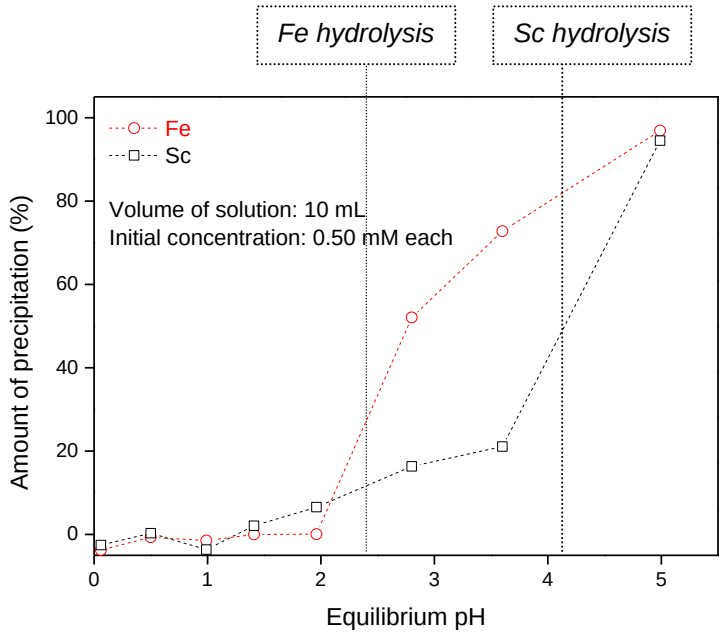

Figure 7: Amount of precipitation as a function of the pH - binary mixture (nitrate medium)

One can clearly see that Fe(III) hydrolysis takes place at lower pH values than Sc(III). The theoretical pH value at which Fe(III) would precipitate at this concentration is at pH 2.40. For Sc(III), this is at pH 4.10. Figure 7 also shows that the Sc(III) content reduces from the moment the Fe(III) starts to precipitate. This is probably a consequence of co-precipitation with Fe(III). Since the Fe(III) content in red mud is much higher than the Sc(III) content and since this is not the case in the batch experiments which have been performed in order to quantify the hydrolysis reactions, these results raise the questions whether the Sc(III) also gets co-precipitated in the same amount when the pH of the red mud leachates are adjusted. It is expected that all of the Sc(III) will get lost by getting co-precipitated with the Fe(III) precipitation products. It was therefore concluded that optimization of the pH conditions only will probably not be sufficient to obtain significant selectivity for Sc(III) towards Fe(III).

To visualize the Fe(III) and Sc(III) adsorption by DTPA-chitosan-silica from a binary mixture, both the adsorption curve and the hydrolysis curve of Fe(III) and Sc(III) have been combined into one graph, Figure 8. In order for the figure not to be too crowded with text, the experimental details are not shown in the figure. An adsorbent mass of 25.0 mg has been used, the volume of the solution was 10 mL, the initial concentration of each ion was 0.50 mM and the adsorption lasted for 4 h.

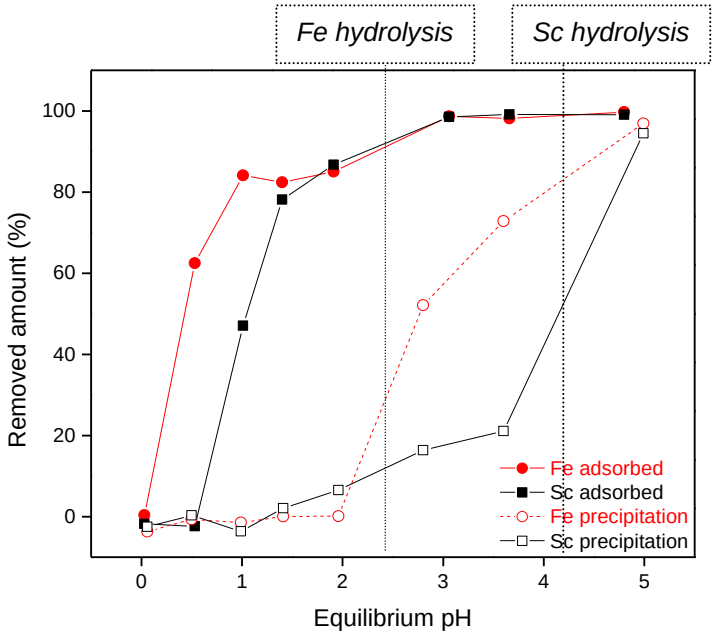

Figure 8: Fe(III) and Sc(III) adsorption and precipitation curve combined in one figure - binary mixture (nitrate medium - DTPA-chitosan silica as adsorbent)

When working at pH 3.00, approximately 60 % of iron has already been precipitated while only 20 % of scandium has precipitated (or co-precipitated). This means that only 40 % of iron had been adsorbed while 80 % of scandium has been adsorbed. This result is quite promising.

6.2.3 Reduction of Fe(III) to Fe(II)

A way to enhance the scandium uptake was to do a preliminary reduction of Fe(III) to Fe(II) before adsorption. Since binding of Fe(II) ions by DTPA is less favorable in comparison with Fe(III) ions, a better selectivity towards Sc(III) ions could be achieved by adsorption with functionalized chitosan-silica. One has to take into account that Fe(II) can reoxidize to Fe(III) in the presence of O_2. In acidic or anaerobic conditions, Fe(II) is quite stable in water but it is better to make sure enough reducing agent is present within the sample.[75] The oxidation of Fe(II) to Fe(III) follows a first order kinetics in terms of Fe(II) and O_2 concentration and a second order kinetics in terms of OH^- concentration for pH values greater than 5.00.[76] For pH values below pH 3.00, the kinetics are independent of the pH value.[76]

A first method to reduce Fe(III) to Fe(II) has been investigated by preparing a 2.50 mM solution of hydroxylamine. Hydroxylamine solution was then added to the Fe(III)/Sc(III) binary solution in order to reduce Fe(III) to Fe(II) according to the following reaction:[77]

$$2\ NH_2OH + 4\ Fe^{3+} \leftrightarrows\ N_2O + 4\ Fe^{2+} + H_2O + \mathbf{4\ H^+} \qquad (3)$$

Since the thermodynamics of the reaction aren't beneficial in an acidic environment, due to the protons within the right lid (K <<< 1), this method was not considered useful in our system for the reduction of Fe(III) to Fe(II). Moreover, hydroxylamine is a rather harmful product.

Another possibility to reduce Fe(III) to Fe(II) is by adding Fe powder to the mixture.[78] The following comproportionation reaction will occur:

$$Fe + 2\ Fe^{3+} \rightarrow 3\ Fe^{2+} \qquad (4)$$

This method, however, is not practical as bringing more ions into solution should better be avoided since these extra ions contaminate the adsorbent surface which implies that saturation of the surface will occur with non-target ions. Also, the Fe powder should be exactly in stoichiometric quantities in order to achieve an easy calculation afterwards. An easy calculation could be achieved when the excess of Fe powder is filtrated, but then oxidation of Fe(II) due to the presence of O_2 will occur and the measurements will become inaccurate. Also A variation on this method is using Zn powder instead of Fe powder. The addition of Zn powder also results in the reduction of Fe(III) to Fe(II). When the Zn was added, the solution became yellowish after a few minutes. Since hydrolysis of Zn is not significant at such low pH values, the yellow color had to be due to the hydrolysis of the Fe(III) ions. After literature search, an explanation was found that Zn in diluted nitric acid reacts according to following reaction:[79]

$$Zn + 2\ HNO_3 \rightarrow Zn(NO_3)_2 +\ H_2 \qquad (5)$$

Since protons are consumed within this reaction for the formation of hydrogen gas, the acidity of the solution decreases, which results in an increase of the pH of the solution. Due to the increase of the pH, hydrolysis of Fe(III) ions occurs and the color of the solution becomes yellow. This estimation has also been double-checked by adding some Zn powder to the binary stock solution (of Fe(III) and Sc(III)). The yellowish color was observed again, besides some tiny bubbles present at the surface of the Zn powder,

which indicates the formation of H_2 gas. Also, the pH had increased to a value of 5.00-6.00. Therefore, this approach was not considered very useful.

A third method to reduce Fe(III) to Fe(II) is by adding sodium sulfite to the solution.[80] Na_2SO_3 is a cheap chemical and considered safe. Moreover, contamination with other metal ions could be avoided with this method. On the other hand, the formation of H_2SO_3 has to be avoided, since this would decompose in SO_2 gas. That is why the pH should be higher than 2.00 when using this method. When working at a pH value of 2.00, the formation of H_2SO_3 is limited.[81] Following reactions will take place:

$$2\ SO_3^{2-} + \mathbf{2\ H^+} \leftrightarrows\ 2\ HSO_3^- \quad (6)$$

$$2\ Fe^{3+} + 2\ HSO_3^- \rightarrow 2\ Fe^{2+} + S_2O_6^{2-} + \mathbf{2\ H^+} \quad (7)$$

Overall reaction: $2\ SO_3^{2-} + 2\ Fe^{3+} \rightarrow S_2O_6^{2-} + 2\ Fe^{2+}$ (8)

Every coefficient of the first reaction is multiplied by two to indicate the similarities between the reactions. As can be seen, the pH of the solution should stay at the same value when using equimolar amounts of Na_2SO_3. Due to the fact that reduced iron can again react with O_2 (dissolved in water), addition of an excess of Na_2SO_3 is necessary. However, when an excess of Na_2SO_3 is added, the equilibrium of the first reaction will shift to the right which results in a pH increase. This pH increase may result in hydrolysis of Sc(III). Conclusion: an excess of Na_2SO_3 is needed but the pH value may not exceed pH 4.00 since hydrolysis of Sc(III) will occur at pH values higher than 4.00.

The molarity, of the Na_2SO_3 solution which will be used in feature experiments, has been determined by adding a different amount of a Na_2SO_3 solution (with a known concentration) to 2 mL of the binary Fe(III)/Sc(III) mixture and diluted with Milli-Q water till 10 mL. A yellow color was an indication of hydrolysis and therefore indicated a too high concentration of Na_2SO_3. The presence of Fe(III) ions could easily be detected by adding KSCN to the solution. If the solution turned red, Fe(III) ions were still present which indicated that the Na_2SO_3 concentration was too low. In this way, an optimum could be determined. The optimum Na_2SO_3 concentration was determined to be 0.04 M.

Since all of the Fe(III) ions are reduced to Fe(II) when using this method, the results won't be any different when using solutions of different pH values. The only conditions which have to be fulfilled concerning the pH are not to exceed pH 4.00 (hydrolysis of

Sc(III)) and not to go below pH 1.00 (the adsorbent does not adsorb well at very low pH values). Just to make sure, an experiment has been conducted where the pH influence is investigated.

The reduction of Fe(III) to Fe(II) has been performed by adding 8 mL of a 0.05 M Na_2SO_3 solution to 2 mL of the binary mixture. In order to determine whether the Na_2SO_3 keeps the Fe(III) reduced to Fe(II) during the 3 h lasting experiment, a test experiment has been conducted by imitating the same reaction conditions as within the actual adsorption experiments. The Fe(III) absence has been proved by adding a little bit of KSCN to the solution. As no color change from colorless to red was observed, it could be concluded that still no Fe(III) was present in the solution.

The reduction of Fe(III) using Na_2SO_3 gave good results. Figure 9 shows the amount of Fe(III) and Sc(III) ions which have been removed from the solution (either by hydrolysis or adsorption). As can be seen, the reduction of Fe(III) to Fe(II) has got a positive effect on the selectivity of the DTPA-chitosan-silica towards scandium. The trend of the removed amount of iron is not as smooth as the trend of the data points of Sc(III) due to the fact that more processes take place with the iron: Fe(III) and Fe(II) adsorption onto the adsorbent, Fe(III) and Fe(II) hydrolysis, Fe(III) reduction by Na_2SO_3 and Fe(II) oxidation by air. Around pH 1.00, there seems to be a little decrease in iron concentration (which is being reflected onto Figure 9 by an increase of the amount removed from solution). This could be explained by the fact that at low pH values, the reduction of Fe(III) to Fe(II) using Na_2SO_3 does not proceed as good as at somewhat higher pH values (more H_2SO_3 and HSO_3^- and less SO_3^{2-} will be present).

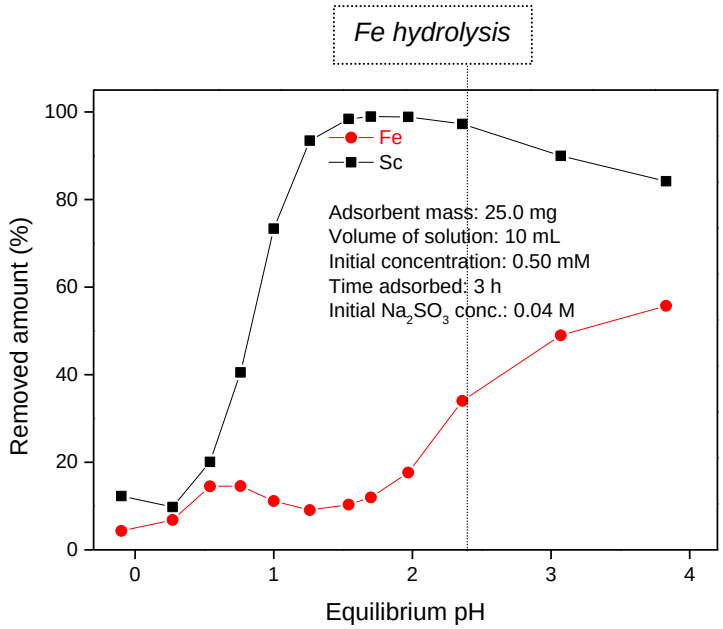

Figure 9: Removed amount of ions out of the solution after Fe^{3+} reduction took place using Na_2SO_3 (nitrate medium - DTPA-chitosan-silica as adsorbent)

Also, a decrease in adsorption amount of Sc(III) is observed when the pH is raised from 1.50 to 4.00. This can be explained by the fact that sulfite forms a colloidal precipitation with rare-earth elements (scandium in specific). This colloidal precipitation would crystallize and precipitate after a while but as long as this has not occurred, the Sc(III) remains in solution (as colloidal precipitation) which implies that it can be measured with the TXRF apparatus. The formation of this colloidal suspension increases with increasing pH since more H_2SO_3 is converted to HSO_3^- and SO_3^{2-}. These colloids have very little affinity for the DTPA ligand since the Sc(III) ion is already coordinative saturated. This results in a decrease in adsorption amount for Sc(III) with increasing pH. However, at pH 2.00, the selectivity towards Sc(III) ions is magnificent as nearly 100 % of the Sc(III) ions are adsorbed while only 20 % of Fe(III) ions are removed from solution.

6.2.4 Red mud samples

Both the red mud HNO_3 leachates and HCl leachates have been studied by doing some adsorption experiments onto the red mud solutions. First, the red mud leachate was filtrated in order to remove the red colored sediment within the red mud sample. This has

been done by first removing most of the particles using a standard paper filter after which the last particles were separated by centrifugation and decantation.

Since the reduction of Fe(III) to Fe(II) using Na_2SO_3 gave quite good results, this method has also been applied to the red mud leachates, in combination with using DTPA-chitosan-silica as an adsorbent. Since the red mud leachates contain a huge amount of different elements, analysis by TXRF was not possible due to spectral overlap of several peaks. For instance, the calcium K_β spectral line (calcium has a concentration of approximately 1000 ppm) on the TXRF spectrum interferes with the K_α spectral lines of scandium (which has only got a concentration of 1 - 2 ppm) and the K_α spectral lines of titanium interfere with the K_β spectral line of scandium. Moreover, it is not possible to measure sodium, aluminium and silicon with TXRF, because of instrumental limitations that result from the low X-ray yields for these light elements. Therefore, all of the concentration levels concerning the adsorption experiments on the red mud leachates were quantified using ICP-MS.

Since Na_2SO_3 is added in order to reduce Fe(III) to Fe(II), Na has not been included in the graphs. A varying amount of Na_2SO_3 and 25.0 mg of DTPA-chitosan-silica has been added to the red mud leachates. The adsorption lasted 3 h. The graph of the red mud HNO_3 leachate is shown within Figure 10 and the graph of the red mud HCl leachate is shown within Figure 11.

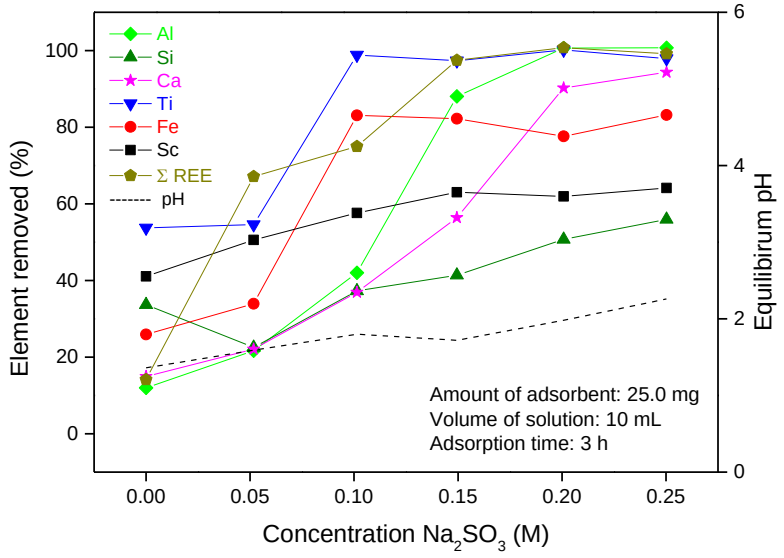

Figure 10: Influence of sulfite concentration on adsorption of elements within HNO_3 red mud leachate (DTPA-chitosan-silica as adsorbent)

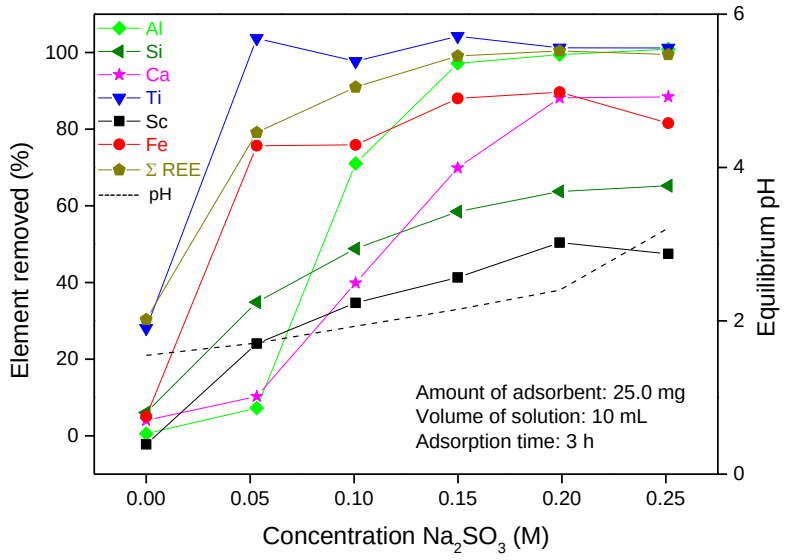

Figure 11: Influence of sulfite concentration on adsorption of elements within HCl red mud leachate (DTPA-chitosan-silica as adsorbent)

It is observed that the pH increased by adding more Na_2SO_3. This is due to the fact that protons are consumed when Na_2SO_3 is added to the solution. When more and more Na_2SO_3 is added to the solution, the equilibrium will shift more and more towards the HSO_3^- form which implies a consumption of protons and an increase in pH. The Fe(III) is reduced to Fe(II) and this sets back free an equimolar amount of protons (see equation 6 on page 41). The pH values are important data since hydrolysis of different elements can take place at somewhat higher pH values.

As can be seen, the adsorption characteristics concerning the HNO_3 red mud leachate and the HCl red mud leachate are quite similar. The total percentage of scandium adsorption is a bit higher at every concentration level of Na_2SO_3 but at these concentration levels of 1 - 2 ppm of scandium, errors can be quite significant. Unfortunately however, the method with Na_2SO_3 in order to reduce Fe(III) to Fe(II), does not seem to work on realistic red mud leachates. This is probably due to the great variety of other elements present within the red mud leachates, which can be preferentially adsorbed to the DTPA-chitosan-silica.

6.3 Non-functionalized chitosan-silica as adsorbent

Instead of using functionalized chitosan-silica particles, non-functionalized chitosan-silica can be used. The mechanisms which have been discussed so far, involve cation exchange onto negatively charged carboxylate groups. The mechanism regarding the use of non-functionalized chitosan-silica particles however, is totally different. Instead of the cation exchange mechanism, anion exchange is considered. The sulfate ions form negative complexes with the rare-earth elements. For example, the major species present within a sulfate scandium solution is *fac*-$[Sc(SO_4)_3(OH_2)_3]^{3-}$.[82] These negative complexes can then be exchanged on the positively charged amine groups of the non-functionalized chitosan-silica. This implies that a more negative pH value, which also means more positively charged amine groups, will result in a greater adsorption of the rare-earth elements. Hopefully, the selectivity towards Sc(III) can be enhanced using this method.

The data of the experiments with non-functionalized chitosan-silica (within sulfate medium) was rather hard to quantify. The values of the TXRF measurements were not consistent to one another, even when the same glass carrier was measured twice significant differences in scandium or iron content were observed. This is probably due to the presence of the salt within the sulfate solutions, which results in matrix effects on the sample carriers surface. That is why the sample preparation of the glass carriers is extremely important. In order to check which sample preparation technique worked best, some different parameters were studies (the use of different standards, the volume of the sample droplet, the use of Serva or not and the drying temperature). The sample preparation method which gave the best results was using a Ce standard for the determination of the Sc content and using a Ho standard for the determination of the Fe content, using a sample droplet of 2 µL, using Serva and drying the sample carriers at 90 °C. Serva is used to make the sample carrier more hydrophobic, which results in a nice droplet of sample.

The results of the pH influence on the adsorption amount are shown within Figure 12. A sulfate concentration of 0.40 M has been used since this concentration has been determined to be the most efficient in order to adsorb the scandium selectively over the iron.

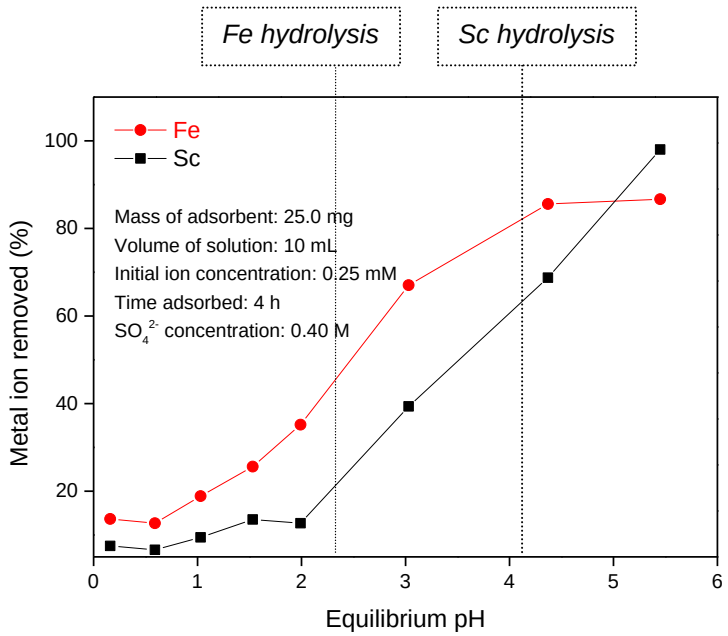

Figure 12: pH influence on the adsorption characteristics of a binary Fe(III)/Sc(III) mixture (sulfate medium - non-functionalized chitosan-silica as adsorbent)

As can be seen within Figure 12, the difference between the Fe(III) adsorption compared to the Sc(III) adsorption is not beneficial for the main goal to be achieved (as much adsorption of scandium as possible and as less adsorption of iron as possible). For example, at pH 2.00, about 35 % of the initial iron content has been adsorbed by the chitosan-silica while only 10 % of scandium has been adsorbed. Since the TXRF measurements were not consistent enough, the concentration levels were measured again using ICP-MS. The values used within Figure 12 are the ones corresponding to the ICP-MS measurements. A conclusion could be made that the adsorption within sulfate medium, using non-functionalized chitosan-silica as an adsorbent, is not the method we hoped for in order to obtain selectivity for scandium.

6.4 EGTA-chitosan-silica as adsorbent

It was rather hard to gain significant selectivity differences when using DTPA-chitosan-silica or non-functionalized chitosan-silica as an adsorbent and by changing external parameters such as the addition of reductantia, changing the pH or changing the counter-ion. That is why the chitosan-silica was functionalized with another functionality, namely EGTA. As shown in Table 4, the Sc(III) adsorption is favored over Fe(III) when

using EGTA-chitosan-silica because the stability constants of Sc(III) with EGTA (log K = 25.40) is way higher than the stability constant of Fe(III) with EGTA (log K = 20.50). The selectivity towards Sc(III) is expected to be enhanced when immobilizing EGTA on chitosan-silica and using this EGTA-chitosan-silica as an adsorbent. Nd(III) is considered a model ion for the REEs.

Table 4: List of popular ligands and their stability constants (log K) with Sc(III), Fe(III) and Nd(III)[73,74]

	Sc(III)	**Fe(III)**	**Nd(III)**
EDTA	23.10	25.10	16.61
DTPA	27.43	28.60	21.60
EGTA	25.40	20.50	16.28
NTA	12.70	15.87	11.26
CyDTA	25.40	28.05	17.69
DHEG	8.00	?	7.60

6.4.1 Synthetic solutions

First, the single-element solutions of scandium and iron were studied by taking 10 mL of a 0.50 mM Sc(III) or Fe(III) nitrate solution, adjusting the pH values by adding HNO_3 or NaOH and adding 25.0 mg of EGTA-chitosan-silica to the solutions. The adsorption was carried out for 4 h. The adsorption of iron and scandium was investigated with EGTA-functionalized chitosan-silica as a function of pH (Figure 13).

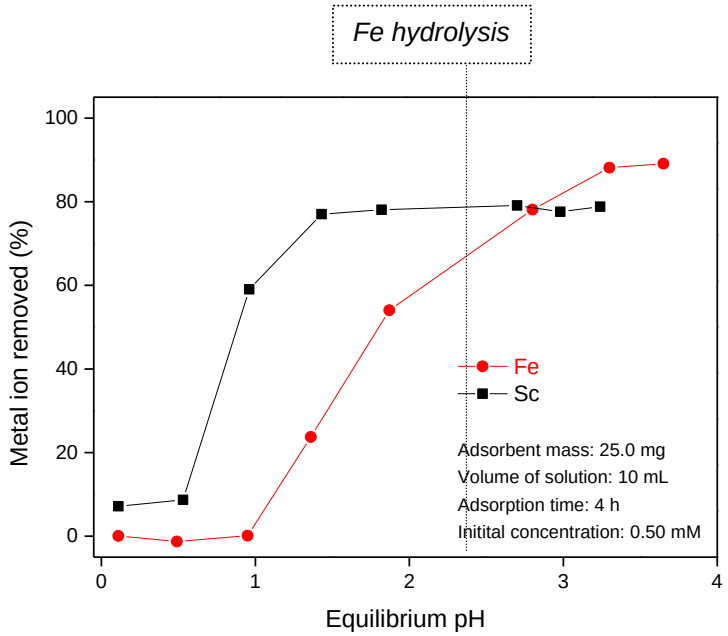

Figure 13: pH influence on adsorption characteristics of single element solutions (nitrate medium - EGTA-chitosan-silica as adsorbent)

As can be seen, the Sc(III) gets adsorbed at lower pH values than Fe(III). When DTPA-chitosan-silica was used, the reverse was true. Our hypothesis seems to be confirmed in a way that Sc(III) is favored over Fe(III) by using EGTA-chitosan-silica as adsorbent. This is a major breakthrough in the thesis project since this enables the possibility of adsorbing the Sc(III) at pH values at which Fe(III) is no longer adsorbed (or at least no significant amount). Only 80 % of the Sc(III) is adsorbed to the EGTA-chitosan-silica when using 25.0 mg of adsorbent. This indicates a lower adsorption capacity of these materials.

In order to investigate the selectivity differences between the Fe(III) and Sc(III) adsorption by EGTA-chitosan-silica, also a batch experiment has been conducted with a binary Fe/Sc solution. The same reaction setup has been used. The results are shown within Figure 14.

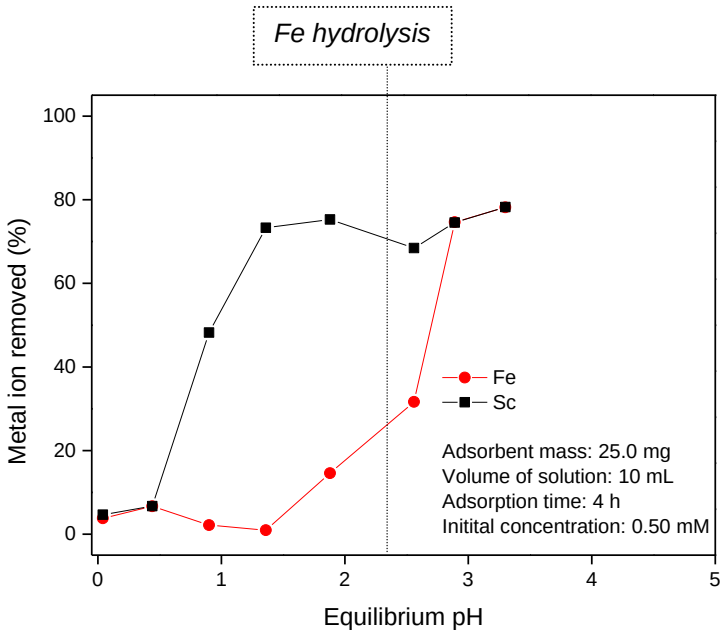

Figure 14: pH influence on adsorption characteristics of a binary solution (nitrate medium - EGTA-chitosan-silica as adsorbent)

From Figure 14, it can be observed that the selectivity increased in the binary mixture of iron and scandium, compared to the respective single-element solutions. This is probably due to the competition between the Sc(III) and Fe(III), which is a consequence of the limited number of available adsorption sites. In the single element solutions, no competing Sc(III) ions were present in the adsorption study of Fe(III), explaining why the corresponding adsorption amount was higher in that experiment.

6.4.2 Red mud samples

The adsorption characteristics of the pH influence onto the red mud samples have been studied using EGTA-chitosan-silica in a batchwise manner. Batch experiments have been conducted by taking 10 mL of a HNO_3 or HCl red mud leachate, adjusting the pH values by adding some HNO_3 or HCl respectively in order to decrease the pH or by adding NaOH to increase the pH. 25.0 mg of EGTA-chitosan-silica is then added to the batches and adsorption has been carried out for 4 h. The leachates were then filtered using a 0.45 µm polypropylene syringe filter after which the elemental content was measured. Analysis of concentrations was done by ICP-MS. Figure 15 represents the

adsorption of the HNO_3 red mud sample by EGTA-chitosan-silica while Figure 16 corresponds to the adsorption of the HCl red mud sample by EGTA-chitosan-silica.

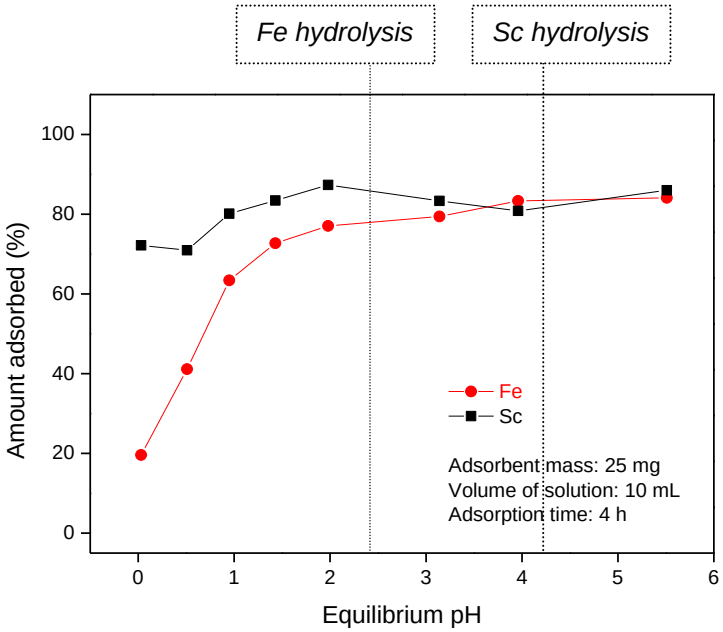

Figure 15: pH influence on adsorption characteristics of HNO_3 red mud leachate (EGTA-chitosan-silica as adsorbent)

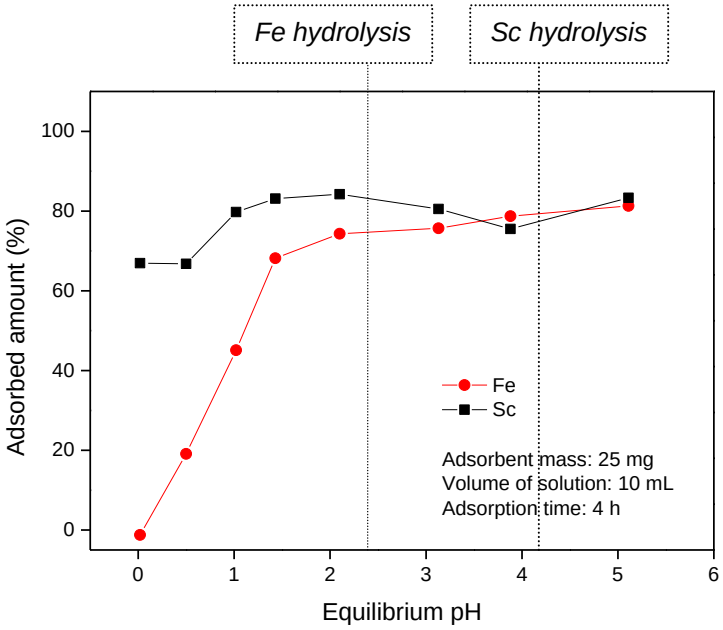

Figure 16: pH influence on adsorption characteristics of HCl red mud leachate (EGTA-chitosan-silica as adsorbent)

The adsorption of Sc(III) is favored, both for the HNO_3 red mud leachate as for the HCl red mud leachate. Since this is the case, the EGTA-chitosan-silica will be used in a column setup for the selective separation of the elements within the red mud samples.

6.5 Stripping efficiency and reusability

Since the EGTA-chitosan-silica is determined to be the most successful adsorbent to selectively separate scandium from iron, this adsorbent will be used from now on. Before conducting the column experiments, the stripping efficiency and the reusability were studied. Since a minimum level of acid consumption is preferred in order to strip the adsorbent, the difference in stripping efficiency with different molarities of the HNO_3 stripping solution was studied. The adsorption experiments are conducted by adding 25.0 mg of EGTA-chitosan-silica to 10 mL of a 0.50 mM Sc solution and adsorbing for 3 h. The adsorption amount is measured by measuring the scandium content within the aqueous solution using TXRF. The adsorbent particles, containing Sc(III), are then washed with 10 mL MilliQ water and stripped by adding HNO_3 solutions of different molarities (0.00 M, 0.25 M, 0.50 M, 0.75 M, 1.00 M, 1.25 M, 1.50 M, 1.75 M and 2.00 M). The duration of the stripping step was 1 h. The scandium content within the HNO_3 strip solutions are then measured in order to determine the stripping efficiency. Figure 17 shows the stripping efficiency as a function of the molarity of the HNO_3 stripping solution.

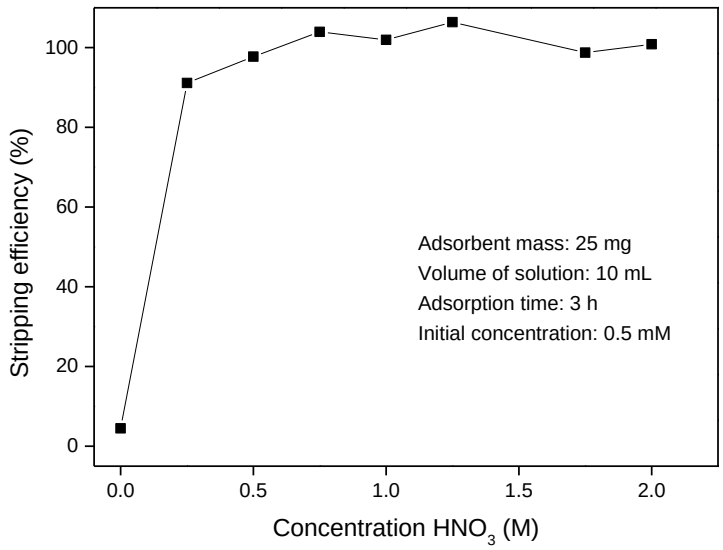

Figure 17: Scandium stripping efficiency as a function of HNO_3 concentration (nitrate medium - EGTA-chitosan-silica as adsorbent)

To ensure complete stripping, a minimum concentration level of the HNO_3 solution is necessary. Since the stripping seems to be nearly quantitative by addition of 0.75 M HNO_3, it was therefore decided that the concentration level of the HNO_3 stripping solution needed to be 1.00 M.

The reusability of the EGTA-chitosan-silica is also an important parameter. In order to investigate the reusability, adsorption was performed by adding 25.0 mg of EGTA-chitosan-silica to 10 mL of a 0.50 mM Sc(III) solution. After the 3 h lasting adsorption, the mixture is centrifuged at 5000 rpm for 10 min. The scandium content within the decantate is measured using the TXRF apparatus. After the centrifuge step, the EGTA-chitosan-silica is washed by adding 10 mL of milliQ to the particles. The EGTA-chitosan-silica is separated from the liquid by centrifuging. Afterwards, the loaded EGTA-chitosan-silica is stripped by adding 10 mL of a 1.00 M HNO_3 solution and stripping for 1 h. The scandium content within the stripping solution is measured by using the TXRF apparatus. Before reusing the adsorbent, the EGTA-chitosan-silica particles are washed 3 times by adding 10 mL of milliQ water in order to remove all the stripping solution and in order to neutralize the pH of the particles. This process is repeated 7 times in total. The results are plotted in Figure 18.

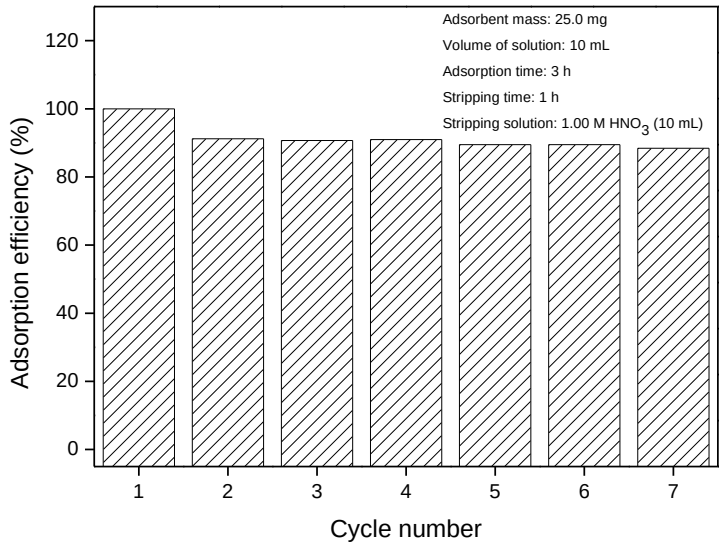

Figure 18: Reusability of EGTA-chitosan-silica (Sc(III)nitrate solution)

As can be seen, the adsorption efficiency is quite good. After the first cycle, the efficiency drops to about 90 %, but after the following cycles, the adsorption efficiency remains at the same percentage. Also, the stripping of the adsorbent was varying from 90 % to 100 % stripping efficiency. This implicates that the adsorbent can definitely be used multiple times within a column stripping setup.

7 COLUMN EXPERIMENT

For the column experiment, the red mud leachate within nitrate medium will be used. 1.5 g of EGTA-chitosan-silica and 1.5 g of pure silica was packed into a column and the bearings were sealed using teflon tape in order to prevent leakages. The additional silica was needed since the eluens did not percolate well through the EGTA-chitosan-silica. A maximum pressure of 15 bar was set, but most of the time the pressure was around 3 bar.

Before the adsorption of the metals within the red mud leachate could take place, the column was washed using MilliQ water. Then, the column was set at pH 2.00 before the red mud leachate was added. After adding the red mud (nitrate) leachate, the metals were stripped from the column by elution with solutions that were gradually acidified with HNO_3. This way, a decreasing pH gradient was applied. 25 mL of each pH solution (ranging from pH 2.00 to pH 0.00, in steps of 0.25) was inserted into the column. Elution fractions of 5.0 mL were collected. The elution rate was 37 mL/h and a total of 43 fractions was obtained. The pH of the fractions was measured to be able to follow up the process. After a separation experiment, the column can be stored by rinsing the column with milliQ water. This prevents oxidation of the column by residuals of HNO_3. The chromatogram resulting from the separation experiment is shown within Figure 19. The dashed line corresponds to the equilibrium pH.

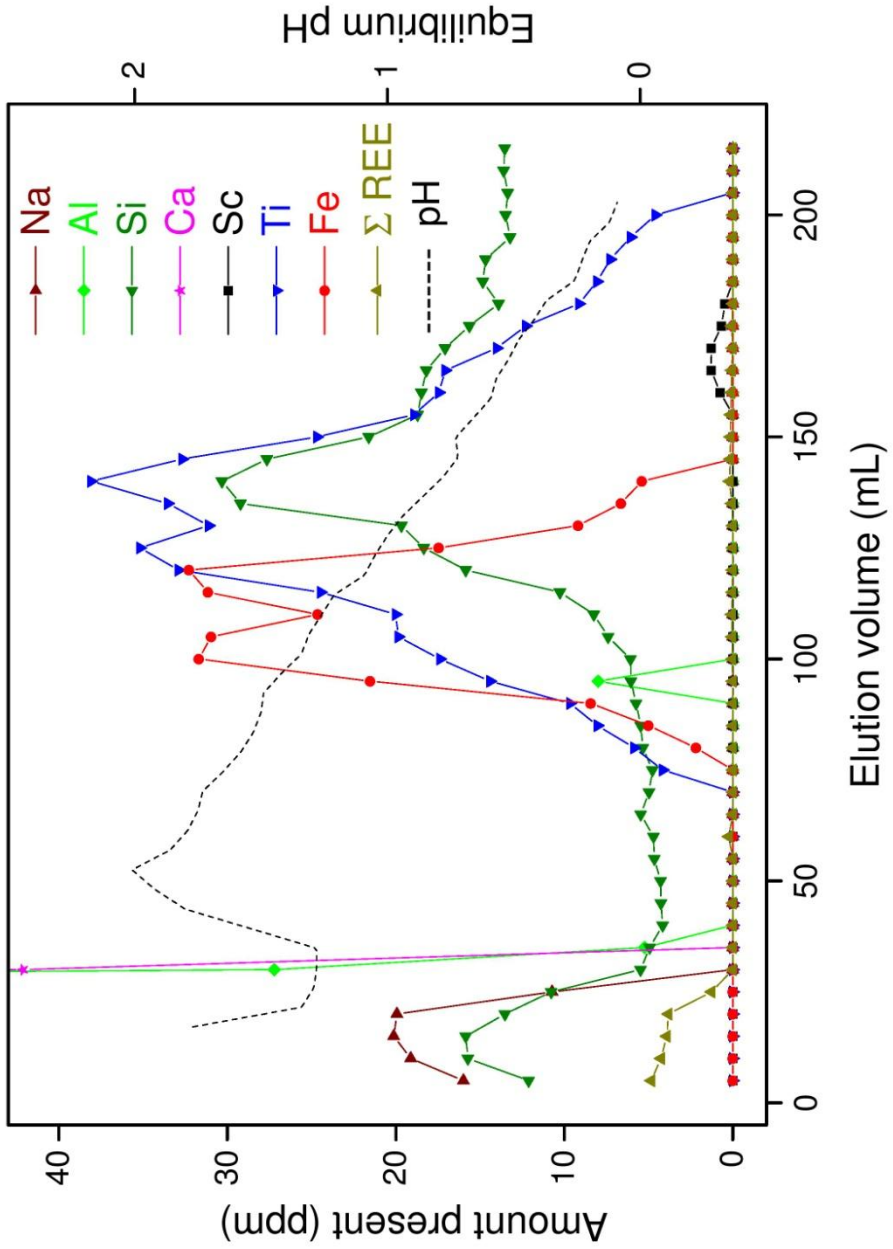

Figure 19: Separation of the elements within a red mud sample using a column setup (nitrate medium - EGTA-chitosan silica as adsorbent)

As can be seen, the iron is separated from the scandium by performing the column experiment using EGTA-chitosan-silica as adsorbent. Fraction 32 to 36 contain scandium, which corresponds to pH 0.66 - 0.48. A small disadvantage is that scandium does not elute in pure form from the column. Titanium and silicium are also present within the fractions containing the scandium. This, however, can be overcome by adjusting the experimental conditions. As can be seen, most of the titanium and silicium elutes at higher pH values (which is earlier in time). If the elution rate is decreased, an even better separation of the elements will be achieved. Another possibility is to

gradually decrease the pH and just before scandium would elute, the pH is kept steady in order to remove all of the other elements before stripping the scandium. Also, using a longer column results in a better separation of the elements. The type of stripping solution can also be an important factor. If a stripping solution with a softer character (such as a thioureum-solution) is used, maybe the selectivity is enhanced even more since scandium has got a hard character.

If there are still some impurities present within the scandium fraction after considering all of the previous elements, some of the water content of the fractions can be evaporated (in order to gain a higher scandium concentration) and after adding oxalic acid, $Sc_2(C_2O_4)_3 \cdot 5H_2O$ will be formed and scandium will selectively be precipitated. In this way, the scandium fraction is purified.

8 CONCLUSIONS

The main goal of this master thesis project was the separation of scandium out of a red mud sample. The focus of this thesis project was to separate scandium from iron. The biggest challenges were their similar ionic radius and therefore their resembling characteristics and the fact that iron is present in way greater concentration levels in red mud compared to scandium. Compared to other methods to separate scandium from the other elements present within bauxite residue, the developed method within this master thesis has got some advantages. Chitosan is a low-cost biological material derived from waste material, which makes using chitosan-based adsorbents an interesting feature in terms of economics.

Considering the three types of adsorbents used (non-functionalized chitosan-silica, DTPA-chitosan-silica and EGTA-chitosan-silica), EGTA-chitosan-silica is considered to be the most effective adsorbent. All three adsorbents have been synthesized and characterized. The optimal parameter setting concerning the batch experiments was determined to be using 25.0 mg of adsorbent, letting the adsorption last for 4 h and working at a pH of approximately 2.00. These parameter settings are for a concentration level of 0.5 mM of the target element.

Also, another approach in order to enhance the selective uptake of scandium in comparison with iron was considered by reducing Fe(III) to Fe(II). Some ways have been studied and the best way to do so, is by adding Na_2SO_3 to the solutions. This method gave some promising results.

The adsorbent which gave the most promising results, being EGTA-chitosan-silica, has been used in a column stripping setup. In this way, the elements present within the red mud sample(s) have been separated from one another. The main goal of the master thesis project has therefore been achieved. Also, the reusability (> 90 % efficiency) and the stripping efficiency of the EGTA-chitosan-silica are important factors to consider.

9 REFERENCES

(1) Guibal, E. Interactions of metal ions with chitosan-based sorbents: a review, *Separation and Purification Technology,* **2004**, *38*, 43.

(2) Ochsenkühn-Petropoulou, M. T.; Hatzilyberis, K. S.; Mendrinos, L. N.; Salmas, C. E. Pilot-Plant Investigation of the Leaching Process for the Recovery of Scandium from Red Mud, *Industrial & Engineering Chemistry Research,* **2002**, *41*, 5794.

(3) Massari, S.; Ruberti, M. Rare earth elements as critical raw materials: Focus on international markets and future strategies, *Resources Policy,* **2013**, *38*, 36.

(4) Wang, W.; Pranolo, Y.; Cheng, C. Y. Recovery of scandium from synthetic red mud leach solutions by solvent extraction with D2EHPA, *Separation and Purification Technology,* **2013**, *108*, 96.

(5) Ochsenkühn-Petropulu, M.; Lyberopulu, T.; Parissakis, G. Selective separation and determination of scandium from yttrium and lanthanides in red mud by a combined ion exchange/solvent extraction method, *Analytica Chimica Acta,* **1995**, *315*, 231.

(6) Binnemans, K.; Jones, P. T.; Blanpain, B.; Van Gerven, T.; Yang, Y.; Walton, A.; Buchert, M. Recycling of rare earths: a critical review, *Journal of Cleaner Production,* **2013**, *51*, 1.

(7) Kilby, C. China's Rare Earth Trade: Health and the Environment, *The China Quarterly,* **2014**, *218*, 540.

(8) Castor, S.; Hedrick, J. *Rare Earth Elements*; 7 ed.; SME: Littleton, Colorado, 2006.

(9) P.F.L. Advisors. *Analysis of rare earth elements and rare metal markets*, 2013.

(10) Emsbo, P.; McLaughlin, P. I.; Breit, G. N.; du Bray, E. A.; Koenig, A. E. Rare earth elements in sedimentary phosphate deposits: Solution to the global REE crisis? , *Gondwana Research,* **2015**, *27*, 776.

(11) Binnemans, K.; Pontikes, Y.; Jones, P. T.; Van Gerven, T.; Blanpain, B., In *3rd International Slag Valorisation Symposium* Leuven, 2013.

(12) Smith Stegen, K. Heavy rare earths, permanent magnets, and renewable energies: An imminent crisis, *Energy Policy,* **2015**, *79*, 1.

(13) Duyvesteyn, W. P. C.; Putnam, G. F.; EMC Metals Corporation: Nevada, 2014.

(14) Wang, W.; Pranolo, Y.; Cheng, C. Y. Metallurgical processes for scandium recovery from various resources: A review, *Hydrometallurgy,* **2011**, *108*, 100.

(15) Wang, W.; Cheng, C. Y. Separation and purification of scandium by solvent extraction and related technologies: a review, *Journal of Chemical Technology & Biotechnology,* **2011**, *86*, 1237.

(16) Stewart, D.; *Scandium element facts*. Chemicool: Vol. 2014.

(17) Arbuzov, S. I.; Volostnov, A. V.; Mezhibor, A. M.; Rybalko, V. I.; Ilenok, S. S. Scandium (Sc) geochemistry in coals (Siberia, Russian Far East, Mongolia, Kazakhstan, and Iran), *International Journal of Coal Geology,* **2014**, *125*, 22.

(18) Gambogi, J., US Geological Survey. *Mineral Commodity Summaries: Scandium*, 2015.

(19) Badwal, S. P. S.; Ciacchi, F. T.; Milosevic, D. Scandia–zirconia electrolytes for intermediate temperature solid oxide fuel cell operation, *Solid State Ionics,* **2000**, *136–137*, 91.

(20) Kazlauskas, S.; Kežionis, A.; Kazakevičius, E.; Orliukas, A. F. Charge carrier relaxation and phase transition in scandium stabilized zirconia ceramics, *Electrochimica Acta,* **2014**, *134*, 176.

(21) Choi, Y.-H.; Lee, S.-H.; Wackerl, J.; Jung, D.-H.; Suhr, D.-S.; Choi, S.-Y.; Peck, D.-H. Fabrication of scandia-stabilized zirconia electrolyte with a porous and dense composite layer for solid oxide fuel cells, *Ceramics International,* **2012**, *38, Supplement 1*, S485.

(22) Mineral Prices: rare earth metal pricings: Vol. 2015.

(23) Hind, A. R.; Bhargava, S. K.; Grocott, S. C. The surface chemistry of Bayer process solids: a review, *Colloids and Surfaces A: Physicochemical and Engineering Aspects,* **1999**, *146*, 359.

(24) Ochsenkühn-Petropulu, M.; Lyberopulu, T.; Parrisakis, G. Direct determination of lanthanides, yttium and scandium in bauxites and red mud from alumina production, *Analytica Chimica Acta,* **1994**, *296*, 305.

(25) Borra, C. R.; Pontikes, Y.; Binnemans, K.; Van Gerven, T. Leaching of rare earths from bauxite residue (red mud), *Minerals Engineering,* **2015**, *76*, 20.

(26) Tsakanika, L. V.; Ochsenkühn-Petropoulou, M. T.; Mendrinos, L. N. Investigation of the separation of scandium and rare earth elements from red mud by use of reversed-phase HPLC, *Analytical and Bioanalytical Chemistry,* **2004**, *379*, 796.

(27) Ochsenkühn-Petropulu, M.; Lyberopulu, T.; Ochsenkühn, K. M.; Parissakis, G. Recovery of lanthanides and yttrium from red mud by selective leaching, *Analytica Chimica Acta,* **1996**, *319*, 249.

(28) Roosen, J.; Binnemans, K. Adsorption and chromatographic separation of rare earths with EDTA- and DTPA-functionalized chitosan biopolymers, *Journal of Materials Chemistry A,* **2014**, *2*, 1530.

(29) Repo, E.; Warchol, J. K.; Bhatnagar, A.; Sillanpää, M. Heavy metals adsorption by novel EDTA-modified chitosan– silica hybrid materials, *Journal of Colloid and Interface Science,* **2011**, *358*, 261.

(30) Al-Sagheer, F.; Muslim, S. Thermal and mechanical properties of chitosan/SiO<inf>2</inf> hybrid composites, *J. Nanomaterials,* **2010**, *2010*, 1.

(31) Mati-Baouche, N.; Elchinger, P.-H.; de Baynast, H.; Pierre, G.; Delattre, C.; Michaud, P. Chitosan as an adhesive, *European Polymer Journal,* **2014**, *60*, 198.

(32) Varma, A. J.; Deshpande, S. V.; Kennedy, J. F. Metal complexation by chitosan and its derivatives: a review, *Carbohydrate Polymers,* **2004**, *55*, 77.

(33) Pandis, C.; Madeira, S.; Matos, J.; Kyritsis, A.; Mano, J. F.; Ribelles, J. L. G. Chitosan–silica hybrid porous membranes, *Materials Science and Engineering: C,* **2014**, *42*, 553.

(34) Domard, A.; Rinaudo, M.; Terrassin, C. New method for the quaternization of chitosan, *International Journal of Biological Macromolecules,* **1986**, *8*, 105.

(35) Ponomarev, A. V.; Kholodkova, E. M.; Metreveli, A. K.; Metreveli, P. K.; Erasov, V. S.; Bludenko, A. V.; Chulkov, V. N. Phase distribution of products of radiation and post-radiation distillation of biopolymers: Cellulose, lignin and chitin, *Radiation Physics and Chemistry,* **2011**, *80*, 1186.

(36) Zhou, D.; Zhang, L.; Zhou, J.; Guo, S. Cellulose/chitin beads for adsorption of heavy metals in aqueous solution, *Water Research,* **2004**, *38*, 2643.

(37) Hajji, S.; Younes, I.; Ghorbel-Bellaaj, O.; Hajji, R.; Rinaudo, M.; Nasri, M.; Jellouli, K. Structural differences between chitin and chitosan extracted from three different marine sources, *International Journal of Biological Macromolecules,* **2014**, *65*, 298.

(38) Shahidi, F.; Synowiecki, J. Isolation and characterization of nutrients and value-added products from snow crab (Chionoecetes opilio) and shrimp (Pandalus borealis) processing discards, *Journal of Agricultural and Food Chemistry,* **1991**, *39*, 1527.

(39) Guibal, E. Interactions of metal ions with chitosan-based sorbents: a review, *Separation and Purification Technology,* **2004**, *38*, 43.

(40) Inoue, K.; Yoshizuka, K.; Ohto, K. Adsorptive separation of some metal ions by complexing agent types of chemically modified chitosan, *Analytica Chimica Acta,* **1999**, *388*, 209.

(41) Liu, Y.; Cao, X.; Hua, R.; Wang, Y.; Liu, Y.; Pang, C.; Wang, Y. Selective adsorption of uranyl ion on ion-imprinted chitosan/PVA cross-linked hydrogel, *Hydrometallurgy,* **2010**, *104*, 150.

(42) Rinaudc, M.; Pavlov, G.; Desbrières, J. Solubilization of Chitosan in Strong Acid Medium, *International Journal of Polymer Analysis and Characterization,* **1999**, *5*, 267.

(43) Brown, P. L.; Ellis, J.; Sylva, R. N. The hydrolysis of metal ions. Part 6. Scandium(III), *Journal of the Chemical Society, Dalton Transactions,* **1983**, 35.

(44) Aveston, J. Hydrolysis of scandium(III): ultracentrifugation and acidity measurements, *Journal of the Chemical Society A: Inorganic, Physical, Theoretical,* **1966**, 1599.

(45) Smitha, S.; Shajesh, P.; Mukundan, P.; Warrier, K. G. K. Sol-gel synthesis of biocompatible silica-chitosan hybrids and hydrophobic coatings, *Journal of Materials Research,* **2008**, *23*, 2053.

(46) Li, F.; Li, X.-M.; Zhang, S.-S. One-pot preparation of silica-supported hybrid immobilized metal affinity adsorbent with macroporous surface based on surface imprinting coating technique combined with polysaccharide incorporated sol–gel process, *Journal of Chromatography A,* **2006**, *1129*, 223.

(47) Roosen, J.; Spooren, J.; Binnemans, K. Adsorption performance of functionalized chitosan-silica hybrid materials toward rare earths, *Journal of Materials Chemistry A,* **2014**, *2*, 19415.

(48) Rashidova, S. S.; Shakarova, D. S.; Ruzimuradov, O. N.; Satubaldieva, D. T.; Zalyalieva, S. V.; Shpigun, O. A.; Varlamov, V. P.; Kabulov, B. D. Bionanocompositional chitosan-silica sorbent for liquid chromatography, *Journal of Chromatography B,* **2004**, *800*, 49.

(49) Zhao, Z.; Liu, N.; Yang, L.; Wang, J.; Song, S.; Nie, D.; Yang, X.; Hou, J.; Wu, A. Cross-linked chitosan polymers as generic adsorbents for simultaneous adsorption of multiple mycotoxins, *Food Control,* **2015**, *57*, 362.

(50) Božič, M.; Gorgieva, S.; Kokol, V. Homogeneous and heterogeneous methods for laccase-mediated functionalization of chitosan by tannic acid and quercetin, *Carbohydrate Polymers,* **2012**, *89*, 854.

(51) Aljawish, A.; Chevalot, I.; Piffaut, B.; Rondeau-Mouro, C.; Girardin, M.; Jasniewski, J.; Scher, J.; Muniglia, L. Functionalization of chitosan by laccase-catalyzed oxidation of ferulic acid and ethyl ferulate under heterogeneous reaction conditions, *Carbohydrate Polymers,* **2012**, *87*, 537.

(52) Sadeghi-Kiakhani, M.; Arami, M.; Gharanjig, K. Preparation of chitosan-ethyl acrylate as a biopolymer adsorbent for basic dyes removal from colored solutions, *Journal of Environmental Chemical Engineering,* **2013**, *1*, 406.

(53) Połosak, M.; Piotrowska, A.; Krajewski, S.; Bilewicz, A. Stability of 47Sc-complexes with acyclic polyamino-polycarboxylate ligands, *Journal of Radioanalytical and Nuclear Chemistry,* **2013**, *295*, 1867.

(54) Nicolet, T., *Introduction to fourier transform infrared spectroscopy*. Madison, U.S.A., 2001.

(55) Stosnach, H., *S2 Picofox: Total Reflection X-Ray Fluorescence Spectroscopy - Working principles*. Berlin, Germany, 2013.

(56) Iet. Thermo X Series II ICP/MS Data Sheet.

(57) Wolf, R. E. What is ICP-MS? ... And more importantly, what can it do? [Online Early Access]. Published Online: 2005.

(58) Robert, T. A beginner's guide to ICP-MS: part 1. [Online Early Access]. Published Online: 2001. http://www.spectroscopyonline.com.

(59) Fakultät fur chemie. *C/H/N Analysis*. Universität Wien; Vol. 2015.

(60) Thompson, M. CHNS Elemental Analysers. [Online Early Access]. Published Online: 2008.

(61) Fadeeva, V. P.; Tikhova, V. D.; Nikulicheva, O. N. Elemental analysis of organic compounds with the use of automated CHNS analyzers, *Journal of Analytical Chemistry,* **2008**, *63*, 1094.

(62) Govere, E. M. Uncovering the ecosystem secrets. [Online Early Access].

(63) Murali, N., *NMR Spectroscopy: Principles and Applications*, 2010.

(64) Keeler, J. *Understanding NMR Spectroscopy, 2nd Edition*; Wiley, 2010.

(65) Nerz-Storms, M. *The basic nuclear magnetic resonance spectroscopy*. Vol. 2015.

(66) Gottlieb, H. E.; Kotlyar, V.; Nudelman, A. NMR Chemical Shifts of Common Laboratory Solvents as Trace Impurities, *The Journal of Organic Chemistry,* **1997**, *62*, 7512.

(67) Becker, C. E. Methanol poisoning, *The Journal of Emergency Medicine,* **1983**, *1*, 51.

(68) Montembault, V.; Soutif, J.-C.; Brosse, J.-C.; Hilldré, F.; Le Jeune, J.-J. Synthesis of chelating molecules as agents for magnetic resonance imaging, 4 1 . Complexing properties of polycondensates prepared from diethylenetriaminepentaacetic acid bisanhydride, *Reactive and Functional Polymers,* **1997**, *32*, 43.

(69) Zhao, F.; Repo, E.; Yin, D.; Sillanpää, M. E. T. Adsorption of Cd(II) and Pb(II) by a novel EGTA-modified chitosan material: Kinetics and isotherms, *Journal of Colloid and Interface Science,* **2013**, *409*, 174.

(70) Sun, Z.; Liu, Y.; Huang, Y.; Tan, X.; Zeng, G.; Hu, X.; Yang, Z. Fast adsorption of Cd(II) and Pb(II) by EGTA dianhydride (EGTAD) modified ramie fiber, *Journal of Colloid and Interface Science,* **2014**, *434*, 152.

(71) Stefánsson, A.; Seward, T. M. A spectrophotometric study of iron(III) hydrolysis in aqueous solutions to 200 °C, *Chemical Geology,* **2008**, *249*, 227.

(72) Wasikiewicz, J. M.; Nagasawa, N.; Tamada, M.; Mitomo, H.; Yoshii, F. Adsorption of metal ions by carboxymethylchitin and carboxymethylchitosan

hydrogels, *Nuclear Instruments and Methods in Physics Research Section B: Beam Interactions with Materials and Atoms,* **2005**, *236*, 617.

(73) Dojindo; Stability constants: metal chelates

(74) Pniok, M.; Kubíček, V.; Havlíčková, J.; Kotek, J.; Sabatie-Gogová, A.; Plutnar, J.; Huclier-Markai, S.; Hermann, P. Thermodynamic and kinetic study of scandium(III) complexes of DTPA and DOTA: a step toward scandium radiopharmaceuticals, *Chemistry,* **2014**, *23*, 7944.

(75) Schröder, I.; Johnson, E.; De Vries, S. Microbial ferric iron reductases, *FEMS Microbiology Reviews,* **2003**, *27*, 427.

(76) Stumm, W.; Morgan, J. J. *Aquatic Chemistry: Chemical Equilibria and Rates in Natural Waters*; 3 ed., 1995.

(77) Kentucky, U. o. Molecular absorption spectroscopy: Determination of iron with 1,10-phenantroline. [Online Early Access]. Published Online: 2005.

(78) Rourke, W. J.; Lai, W.-C.; Natansohn, S.; GTE Laboratories Incorporated: 1989; Vol. 4,816,233.

(79) Apachitei, I.; Duszczyk, J. Hydrogen evolution, incorporation and removal in electroless nickel composite coatings on aluminium, *Journal of Applied Electrochemistry,* **1999**, *29*, 835.

(80) Millero, F. J.; Gonzalez-Davila, M.; Santana-Casiano, J. M. Reduction of Fe(III) with sulfite in natural waters, *Journal of Geophysical Research: Atmospheres,* **1995**, *100*, 7235.

(81) Sulfite ion, [Online Early Access]. Published Online: 2015. http://www.public.asu.edu/~jpbirk/qual/qualanal/Sulfite.htm

(82) Schrödle, S.; Wachter, W.; Buchner, R.; Hefter, G. Scandium Sulfate Complexation in Aqueous Solution by Dielectric Relaxation Spectroscopy, *Inorganic Chemistry,* **2008**, *47*, 8619.

DEPARTMENT OF CHEMISTRY
MOLECULAR DESIGN AND SYNTHESIS
Celestijnenlaan 200F bus 2404
3000 LEUVEN, BELGIUM
tel. + 32 16 32 74 46
fax + 32 16 32 72 92
Koen.Binnemans@chem.kuleuven.be
www.chem.kuleuven.be